Assessing Calibration Uncertainty in Molecular Dating: The Assignment of Fossils to Alternative Calibration Points

FRANK RUTSCHMANN,[1] TORSTEN ERIKSSON,[2] KAMARIAH ABU SALIM,[3] AND ELENA CONTI[1]

[1]*Institute of Systematic Botany, University of Zurich, Zollikerstrasse 107, CH-8008 Zurich, Switzerland; E-mail: frank@plant.ch*
[2]*Bergius Foundation, Royal Swedish Academy of Sciences, SE-104 05 Stockholm, Sweden*
[3]*Universiti Brunei Darussalam, Department of Biology, Jalan Tungku Link, Gadong BE 1410, Negara Brunei Darussalam*

Abstract.—Although recent methodological advances have allowed the incorporation of rate variation in molecular dating analyses, the calibration procedure, performed mainly through fossils, remains resistant to improvements. One source of uncertainty pertains to the assignment of fossils to specific nodes in a phylogeny, especially when alternative possibilities exist that can be equally justified on morphological grounds. Here we expand on a recently developed fossil cross-validation method to evaluate whether alternative nodal assignments of multiple fossils produce calibration sets that differ in their internal consistency. We use an enlarged Crypteroniaceae-centered phylogeny of Myrtales, six fossils, and 72 combinations of calibration points, termed calibration sets, to identify (i) the fossil assignments that produce the most internally consistent calibration sets and (ii) the mean ages, derived from these calibration sets, for the split of the Southeast Asian Crypteroniaceae from their West Gondwanan sister clade (node X). We found that a correlation exists between *s* values, devised to measure the consistency among the calibration points of a calibration set (Near and Sanderson, 2004), and nodal distances among calibration points. By ranking all sets according to the percent deviation of *s* from the regression line with nodal distance, we identified the sets with the highest level of corrected calibration-set consistency. These sets generated lower standard deviations associated with the ages of node X than sets characterized by lower corrected consistency. The three calibration sets with the highest corrected consistencies produced mean age estimates for node X of 79.70, 79.14, and 78.15 My. These timeframes are most compatible with the hypothesis that the Crypteroniaceae stem lineage dispersed from Africa to the Deccan plate as it drifted northward during the Late Cretaceous. [Biogeography; calibration point; cross-validation; divergence times; fossil calibration; Myrtales; molecular dating; out-of-India.]

The use of DNA sequences to estimate the timing of evolutionary events is increasingly popular. Based on the central idea that the differences between the DNA sequences of two species are a function of the time since their evolutionary separation (Zuckerkandl and Pauling, 1965), molecular dating has been used as a method to investigate both patterns and processes of evolution (Magallón, 2004; Renner, 2005; Rutschmann, 2006; Sanderson et al., 2004; Welch and Bromham, 2005).

However, significant methodological challenges affect the use of molecular dating approaches (Pulquério and Nichols, 2007). Although recent studies have addressed the issue of variation among substitution rates (Aris-Brosou and Yang, 2002; Ho and Larson, 2006; Kishino et al., 2001; Penny, 2005; Rutschmann, 2006; Sanderson, 1997, 2002; Thorne et al., 1998; Yang, 2004), other difficulties persist, especially concerning the calibration procedure (Conti et al., 2004; Lee, 1999; Magallón, 2004; Reisz and Müller, 2004). Calibration consists in the incorporation of independent (nonmolecular) chronological information in a phylogeny to transform relative into absolute divergence times. This information can be based on geological events (e.g., patterns of continental drift, origin of islands and mountain chains) and/or the paleontological record (fossils). Geological calibrations points are assigned to phylogenetic nodes based on the assumption that a geographic barrier caused phylogenetic divergence, thus generating the risk of circular reasoning, if the chronogram derived from the calibration is used to test biogeographical scenarios (Conti et al., 2004; Magallón, 2004). Nevertheless, geological events can provide important validation of dating estimates produced with other types of calibration (e.g., Bell and Donoghue, 2005; Conti et al., 2002; Sytsma et al., 2004).

Although the fossil record is widely regarded as the best source of nonmolecular information about the ages of selected clades (Magallón and Sanderson, 2001; Marshall, 1990b; Sanderson, 1998), several problems plague its use for calibration purposes, including (i) erroneous fossil age estimates, (ii) the idiosyncrasies of fossilization, (iii) the assignment of fossils to specific nodes in a phylogeny, and (iv) the number of fossils used for calibration. In this paper we focus primarily on the two latter aspects of fossil calibration, although all four problems are interrelated.

Erroneous fossil age estimates may depend on misleading stratigraphic correlations or improper radiometric dating (Conroy and van Tuinen, 2003) and the source of the error can only be addressed by improving the geological dating procedures, whereas the effect of the error on molecular dating analyses can be partially addressed by the recently developed fossil cross-validation procedure (Near and Sanderson, 2004; see below).

The idiosyncrasies of the fossilization process may cause the failure of entire species to be preserved or discovered as fossils (Darwin, 1859). This lack of information makes it difficult or impossible to estimate the temporal gaps between the divergence of two lineages, the origin of a synapomorphy, and the discovery of that synapomorphy in the fossil record (see fig. 1 in Foote and Sepkoski, 1999; Magallón, 2004; Springer, 1995). Fossils can thus provide only minimum ages for any lineage, a realization that is now incorporated in dating methods by treating the fossil ages assigned to calibration nodes as upper bounds, rather than fixed constraints (Sanderson
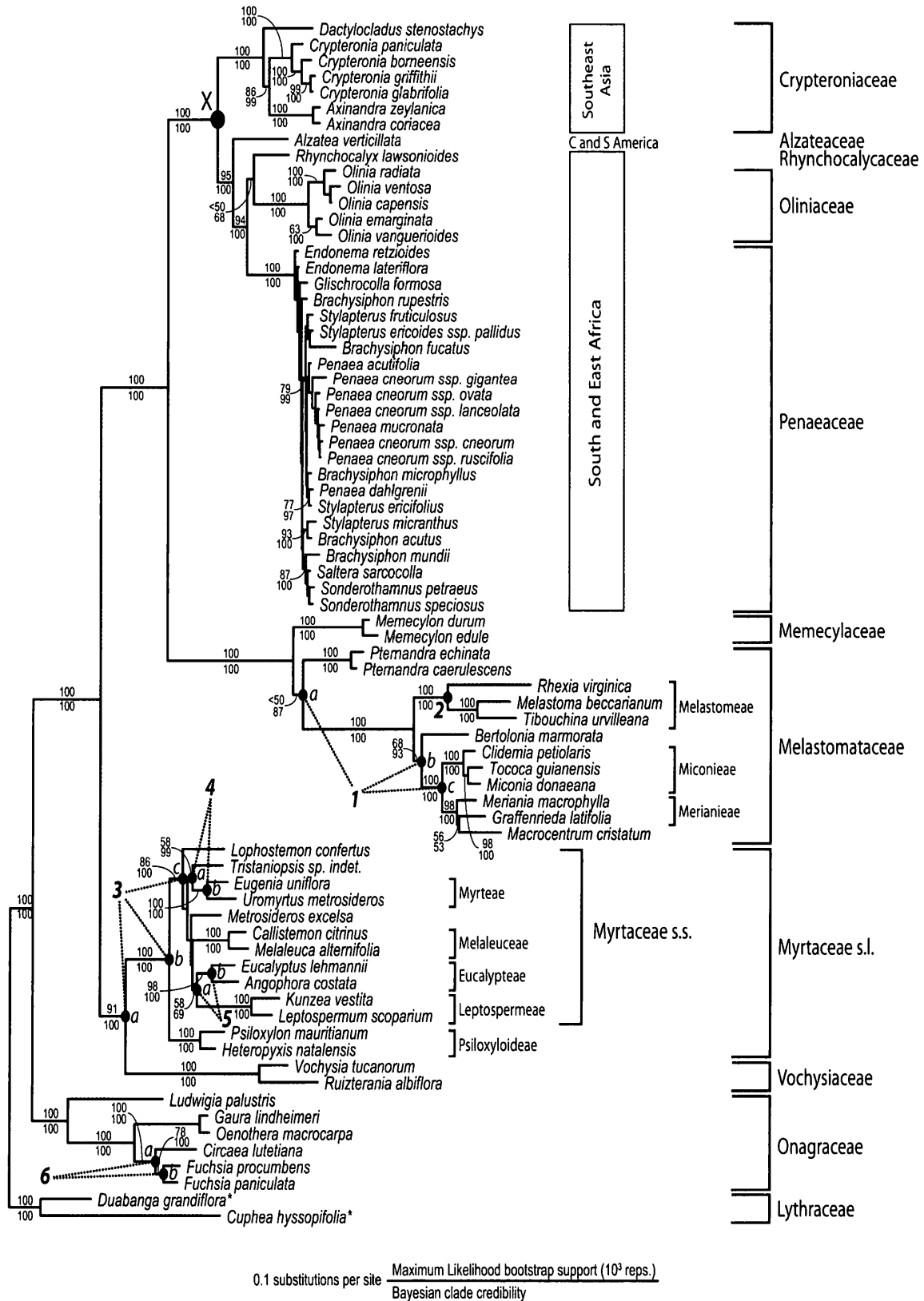
0.1 substitutions per site — Maximum Likelihood bootstrap support (10³ reps.) / Bayesian clade credibility

FIGURE 1. MrBayes majority-rule consensus tree with maximum likelihood branch lengths optimized in *estbranches*, based on the 5124-nucleotide data set. Maximum likelihood bootstrap support values and Bayesian clade credibility values are reported above and below the branches, respectively. General distribution ranges of the focus groups are reported to the right of the tree, as are the infrafamilial ranks relevant to fossil nodal assignments. Node X represents the phylogenetic split between the Southeast Asian Crypteroniaceae stem lineage and its African/South American sister clade. Alternative nodal assignments (*a*, *b*, or *c*) for the six fossils listed in Table 1 (numbers 1 to 6) are labeled on the tree. Outgroup taxa are indicated by an asterisk.

2003; Thorne and Kishino, 2002). Furthermore, recently developed methods attempt to estimate the gap between the time of first appearance of a synapomorphy in the fossil record and the time of divergence between two lineages by assuming that the size of the gap is inversely correlated with the quality and density of the fossil record within a given stratigraphic interval and depends on the rates of origination, extinction, and preservation of the focus lineage (Foote et al., 1999a, 1999b; Marshall, 1990a, 1990b; Tavaré et al., 2002; Yang and Rannala, 2005).

A problem that has received less attention (Pulquério and Nichols, 2007), in spite of having potentially serious effects on nodal age estimates (Conti et al., 2004; Moyle 2004), is the assignment of fossils to specific nodes in a phylogeny. Depending on their preservation state, relative abundance, and the distinctiveness of selected morphological traits, it can be problematic to unambiguously assign fossils to a particular clade in a given phylogeny (Benton and Ayala, 2003; Doyle and Donoghue, 1993). More specifically, it is necessary to determine whether the fossil represents an extinct member of the stem or the crown group of extant taxa (de Queiroz and Gauthier, 1990; Doyle and Donoghue, 1993; Hennig, 1969; Magallón, 2004; Magallón and Sanderson, 2001). Ideally, the assignment would be based on a comprehensive cladistic morphological analysis of both extant and extinct taxa, but, due to their complexity, such analyses remain regrettably rare (Conti et al., 2004; Near et al., 2005b). In practice, assignment of fossils to selected nodes (called "calibration nodes" from now on) is usually based on more intuitive comparisons between the character states of the fossil and the distribution of synapomorphies in the phylogeny. Although this critical step of calibration may be less problematic in certain groups of organisms (e.g., vertebrates), it often represents a considerable challenge in plants, due in part to their open body plan (Donoghue et al., 1989). When a fossil is finally attached to a node, the node in question assumes the age of the fossil, thus becoming a "calibration point."

For the reasons explained above, the use of a single fossil for calibration can produce strongly biased molecular age estimates (Alroy, 1999; Conroy and van Tuinen, 2003; Graur and Martin, 2004; Hedges and Kumar, 2003; Lee, 1999; Reisz and Müller, 2004; Smith and Peterson, 2002; van Tuinen and Hadly, 2003). Additionally, the nodal distance of the calibration point to the node(s) of interest and the root of the phylogeny may strongly influence the estimated ages (Conroy and van Tuinen, 2003; Reisz and Müller, 2004; Smith and Peterson, 2002). Therefore, it seems desirable to use multiple fossils, preferably placed in different clades (Brochu, 2004), for molecular dating purposes, in the hope that the biases built into their assignment to specific calibration nodes may cancel each other out (Conroy and van Tuinen, 2003; Smith and Peterson, 2002; Soltis et al., 2002). Although this approach may not represent the most theoretically satisfying solution to the problem of calibration, it reflects the current limit of the methodological advances on this issue (Pulquério and Nichols, 2007).

Recently developed methods allow for the incorporation of multiple calibration points (termed "multicalibration" from now on) in the dating procedure (Drummond et al., 2006; Kishino et al., 2001; Sanderson, 1997, 2002; Thorne et al., 1998; Yang, 2004; Yang and Rannala, 2005). When multiple fossils are available, it is also possible to use one fossil at a time to generate age estimates for the nodes to which the other fossils are assigned and then compare the estimated ages with the fossil ages at those nodes, essentially leading to an assessment of the consistency among calibration points (Near and Sanderson, 2004; Near et al., 2005b). This procedure, known as fossil cross-validation, allows for the identification and removal of incongruent calibration point(s) and has been applied in molecular dating studies of monocotyledons (where two out of eight fossils were removed; Near and Sanderson, 2004), placental mammals (two out of nine; Near and Sanderson, 2004), turtles (seven out of 17; Near et al., 2005b), centrarchid fishes (four out of 10; Near et al., 2005a), and decapods (no fossils removed; Porter et al., 2005).

To summarize, the process of multicalibration involves two main steps: (i) selection of multiple fossils for calibration; (ii) assignment of each fossil to a specific node in the phylogeny (termed "fossil nodal assignment" from now on). The fossil cross-validation method developed by Near and Sanderson (2004) focuses primarily on the first step by removing fossils that are inconsistent with the other fossils of a calibration set. However, the mentioned procedure does not address the question of whether each fossil is assigned to the most reasonable node, thus preventing the possibility of determining whether the source of inconsistency stems from the wrong nodal assignment of the fossil or from an erroneous estimation of the age of the fossil.

In the study presented here, we expand the fossil cross-validation approach to evaluate whether alternative assignments of available fossils to different calibration nodes produce calibration sets with different levels of internal consistency. Whereas the key idea of the method devised by Near and Sanderson (2004) was to eliminate individual fossils that had already been unequivocally assigned to single calibration points in a multicalibration set, the key idea of our approach is to compare the internal consistencies among entire calibration sets formed by multiple fossils that can be attached to alternative calibration points.

To illustrate the problem of fossil nodal assignment described above, we utilize a Myrtales data set centered on the relationships of Crypteroniaceae and related families (named "Crypteroniaceae phylogeny" from now on). Earlier molecular dating results (Conti et al., 2002, 2004; Rutschmann et al., 2004) suggested a possible Gondwanan origin of these families in the Early to Middle Cretaceous, followed by the dispersal of the Crypteroniaceae stem lineage to the Deccan plate (comprising India and Madagascar) while it was rafting along the African coast, ca. 125 to 84 My (million years) ago (McLoughlin, 2001; Plummer and Belle, 1995; Storey et al., 1995; Yoder and Nowak, 2006), a biogeographic

scenario known as the out-of-India hypothesis (Ashton and Gunatilleke, 1987; Bossuyt and Milinkovitch, 2001; Macey et al., 2000; McKenna, 1973; Morley, 2000). However, the estimated age of the crucial biogeographic node, representing the split between the Southeast Asian Crypteroniaceae and the African/South American sister clade (node X; Fig. 1), ranged from 106 to 141 My (Conti et al., 2002), 62 to 109 My (Rutschmann et al., 2004), 57 to 79 My (Moyle, 2004), and 52 My (Sytsma et al, 2004), depending on gene and taxon sampling, but mostly on the contrasting assignment of selected fossils to different nodes in the Myrtales phylogeny (Conti et al., 2004; Moyle, 2004). Given the controversial nature of calibration, the contradictory calibration procedures previously applied to date the Crypteroniaceae phylogeny, and the availability of multiple fossils in Myrtales, this group of taxa provides an ideal case study to investigate problems of fossil nodal assignment, at the same time attempting to refine the age estimates that are central to the biogeographic history of Crypteroniaceae.

To calibrate the Crypteroniaceae phylogeny we use six fossils (Table 1). Based on the morphological traits preserved in the fossils, five out of the six fossils can each be assigned to two or three different nodes in the phylogeny (Fig. 1; Appendix 1). In total, 72 different combinations of six calibration points are possible, each combination forming a calibration set. Here, we employ an expanded molecular data set and the six fossils to address the following questions: (1) How can the fossil cross-validation procedure be used to assign a fossil to a calibration point that is most internally consistent with the other points in a calibration set? In other words, which fossil assignments produce the calibration sets that are most internally consistent? (2) What are the mean ages for the split between the Southeast Asian Crypteroniaceae and their West Gondwanan sister clade estimated by using the most internally consistent calibration sets? The general goal of our paper is to stir discussion and foster further investigation on the under-studied problem of uncertainty in fossil nodal assignment.

MATERIAL AND METHODS

Taxon and DNA Sampling

Sampling was expanded from published studies (Conti et al., 2002; Rutschmann et al., 2004; Schönenberger and Conti, 2003) to include DNA sequences from three plastid (rbcL, ndhF, and rpl16-intron) and two nuclear (ribosomal 18S and 26S; termed nr18S and nr26S from now on) loci for 74 taxa (see online appendix at http://systematicbiology.org). In total, 270 new sequences were generated for this study. Almost complete taxon sampling was achieved for Crypteroniaceae (seven of 12 species; Mentink and Baas, 1992; Pereira and Wong, 1995; Pereira, 1996), Alzateaceae (one of one species; Graham, 1984), Rhynchocalycaceae (one of one species; Johnson and Briggs, 1984), Penaeaceae (19 of 23 species, plus four subspecies of Penaea cneorum; Dahlgren and Thorne, 1984; Dahlgren and van Wyk, 1988), and Oliniaceae (five of eight species; Sebola and Balkwill, 1999; Tobe and Raven, 1984). The five missing species of Crypteroniaceae, Axinandra alata, A. beccariana, Crypteronia elegans, C. macrophylla, and C. cummingii are either very rare, known only from the type, or collected in now deforested areas; for example, in Kalimantan (Indonesia; Pereira, 1996). DNA extractions from dried vouchers were unsuccessful, because all herbarium specimens of these taxa were treated with ethanol after collection. The four missing Penaeaceae, Stylapterus barbatus, S. dubius, S. sulcatus, and S. candolleanus are also either very rare, occur only in restricted areas, or were collected only once or twice each (Jürg Schönenberger, personal communication). Following Sebola and Balkwill (1999), the three missing Oliniaceae are Olinia discolor, O. rochetiana, and O. micrantha. The sampling of taxa outside Crypteroniaceae, Alzateaceae, Rhynchocalycaceae, Oliniaceae, and Penaeaceae was designed to assign the fossils used for calibration as precisely as possible (see Appendix 1) and to represent clade heterogeneity at the family level (Melastomataceae, Myrtaceae s.l., Vochysiaceae, Onagraceae, Lythraceae), based on published phylogenies (Conti et al., 1996, 1997; Renner, 2004; Sytsma et al., 2004). Phylogenies were

TABLE 1. Fossils used in this study with corresponding ages, locations, and references.

Fossils	Fossil ages	Locations	References
1. Melastomataceae leaves	Early Eocene (53 My)	North Dakota	Hickey, 1977
2. Melastomeae seeds	Miocene (26–23 My)	Russia (Siberia, Tambov region), Belarus, Poland, Germany, Belgium	Dorofeev, 1960, 1963, 1988; Collinson and Pingen, 1992; Dyjor et al., 1992; Fairon-Demaret, 1994; Mai, 1995, 2000
3. Pollen of *Myrtaceidites lisamae* = *Syncolporites lisamae*	Santonian (86 My)	Gabon	Herngreen, 1975; Boltenhagen, 1976; Muller, 1981
4. Fruits and seeds of *Paleomyrtinaea*	Late Paleocene (56 My)	North Dakota	Crane et al., 1990; Pigg et al., 1993
5. Eucalypt-like fruits	Middle Eocene (48 My)	Redbank Plains Formation, Queensland, Australia	Rozefelds, 1996
6. *Fuchsia* pollen *Diporites aspis*	Early Oligocene (33.7–28.5 My)	Australia	Daghlian et al., 1985; Berry et al., 1990, 2004

rooted using representatives of Lythraceae, i.e., *Duabanga grandiflora* and *Cuphea hyssopifolia*, based on the results of global Myrtales analyses (Conti et al., 1996, 1997; Sytsma et al., 2004).

DNA Extractions, PCR, Sequencing, and Alignment

DNA was extracted as described in Rutschmann et al. (2004) and Schönenberger and Conti (2003). Primers from Zurawski et al. (1981), Olmstead and Sweere (1994), Baum et al. (1998), Bult et al. (1992), and Kuzoff et al. (1998) were used to amplify and sequence *rbc*L, *ndh*F, *rpl*16-intron, nr18S, and nr26S, respectively. PCR and sequencing procedures followed the protocols described in Rutschmann et al. (2004). The software Sequencher 4.5 (Gene Codes, Ann Arbor, MI) was used to edit, assemble, and proofread contigs for complementary strands. *Rbc*L, nr26S, and nr18S sequences were readily aligned by eye, whereas *ndh*F and *rpl*16-intron sequences were first aligned using Clustal X 1.83 (Thompson et al., 1997) prior to final visual adjustment with MacClade 4.07 (Maddison and Maddison, 2000).

Phylogenetic Analyses

Plastid (*rbc*L, *ndh*F, and *rpl*16-intron) and nuclear (nr18S, nr26S) partitions were first analyzed separately (results not shown). Because the respective 80% majority-rule consensus bootstrap trees (see below) had no well-supported inconsistencies, plastid and nuclear data sets were combined.

Model selection for each partition was performed in MrAIC 1.4 (Nylander, 2005b), a program that uses PHYML 2.4.4 (Guindon and Gascuel, 2003) to find the maximum of the likelihood function under 24 models of molecular evolution. MrAIC identified the optimal models according to two different selection criteria: the corrected Akaike information criterion (AIC) and the Bayesian information criterion (BIC).

Tree topology and model parameters for each data set were estimated simultaneously using MrBayes version 3.0b4 (Huelsenbeck and Ronquist, 2001; Ronquist and Huelsenbeck, 2003). Bayesian topology estimation used one cold and three incrementally heated Markov chain Monte Carlo chains (MCMC) run for 7×10^6 cycles, with trees sampled every 1000th generation, each using a random tree as a starting point and the default temperature parameter value of 0.2. For each data set, MCMC runs were repeated twice. The first 5000 trees were discarded as burn-in after checking for stationarity on the log-likelihood curves. The remaining trees were used to construct one Bayesian consensus tree and to calculate clade credibility values (Fig. 1).

In addition to the Bayesian clade credibility values (see Fig. 1, numbers below branches), statistical support for individual branches was also calculated by bootstrap resampling using the Perl script BootPHYML 3.4 (Nylander, 2005a; see Fig. 1, numbers above branches). This program first generates 1000 pseudoreplicates in SEQ-BOOT (part of Phylip 3.63; Felsenstein, 2004), then performs a maximum likelihood analysis in PHYML (Guindon and Gascuel, 2003) for each replicate under the selected model of evolution, and finally computes a 80% majority rule consensus tree by using CONSENSE (also part of the Phylip package).

Branch lengths (see Fig. 1) were estimated, based on the topology of the Bayesian consensus tree, by using the program *estbranches* as part of the *multidivtime* Bayesian molecular dating procedure (see below).

Molecular Dating Analyses

All dating analyses described below were performed with *multidivtime* (Kishino et al., 2001; Thorne et al., 1998; Thorne and Kishino, 2002), which uses an MCMC procedure to derive the posterior distributions of rates and times. For the present study, it was important that *multidivtime* allows for multiple calibration windows (in our case six calibration points) and different substitution parameters for each data partition (in our case five different partitions).

The analytical procedure followed the steps described in the "Bayesian dating step-by-step manual" (version 1.5, July 2005; Rutschmann, 2005) and included maximum likelihood branch length optimization with the program *estbranches* (see Fig. 1). In the last step of the dating procedure (see Rutschmann, 2005), the following prior distributions were specified (in units of 10 My, as suggested in the manual): RTTM = 12, RTTMSD = 3, RTRATE and RTRATESD = 0.00815, BROWNMEAN and BROWNSD = 0.0833, and BIGTIME = 13. The first two values, which define the mean and the standard deviation of the prior distribution for the age of the root, were chosen in light of published estimates for the age of the Myrtales crown group (100 to 107 My, Wikström et al., 2001, 2003; 105 My, Magallón and Sanderson, 2005; and 111 My, Sytsma et al., 2004; see also Sanderson et al., 2004). The value for BIGTIME was chosen in order to reflect the estimated age of the oldest eudicot pollen (Doyle and Donoghue, 1993). The age of the eudicots (about 125 My) is one of the firmest dates from the fossil record because of the numerous reports of fossil tricolpate pollen, with no tricolpate pollen appearing before this time.

We ran the Markov chain for at least 5×10^5 cycles and collected one sample every 100 cycles, without sampling the first 8×10^4 cycles (burn-in sector). Initial experiments with 2×10^6 cycles showed no differences, leading us to the conclusion that convergence was reached much earlier. We performed each analysis at least twice with different initial conditions and checked the output sample files to assure convergence of the Markov chain by using the program Tracer 1.3 (Rambaut and Drummond, 2005).

The detailed procedure of fossil selection and assignment to alternative nodes for calibration of the molecular clock is described in Appendix 1. Briefly, six fossils were chosen, five of which could be attached to alternative calibrations nodes, for a total of 72 possible calibration sets.

Finding the Most Internally Consistent Calibration Sets by Using Fossil Cross-Validation

To evaluate whether some of the 72 calibration sets were more internally consistent than others, we implemented the fossil cross-validation procedure of Near and Sanderson (2004) and Near et al. (2005b). Whereas these authors developed the method to identify possibly inconsistent points in a single calibration set, we expanded their approach to compare the internal consistencies of different calibration sets generated by alternative nodal assignments of multiple fossils. Therefore, for each of the 72 calibration sets in our case study, we performed the following steps:

1. We fixed one out of the six calibration points and estimated the ages of the remaining five unconstrained nodes.
2. For each unconstrained node, we then calculated the difference D_i between its estimated and its fossil age. This difference was defined by Near and Sanderson (2004) as an absolute deviation measure $D_i = $ (estimated age − fossil age). Instead, we used the relative deviation measure $D_i = $ (estimated age − fossil age)/fossil age), as suggested in Near et al. (2005b).
3. Then, we calculated SS_χ, the sum of the five squared D_i values (by using equation 2.2 in Near and Sanderson, 2004).
4. The procedure described above (steps 1 to 3) was then repeated 5 times, each time by fixing a different calibration point.
5. Based on the six SS_χ scores obtained above, we calculated the average squared deviation s for the entire calibration set (with equation 2.3 in Near and Sanderson, 2004; see Table 2).

By using this procedure iteratively, we obtained s values for all 72 calibration sets. High values of s would indicate that one or more calibration points in a set are inconsistent with the others, suggesting that the corresponding fossils were erroneously assigned to the respective nodes, whereas low s values would characterize calibration sets with high internal consistency.

In order to account for possible effects related to the molecular dating method (in our case *multidivtime*), the cross-validation experiments were repeated by using penalized likelihood (Sanderson, 2002) implemented in *r8s* (Sanderson, 2003; data not shown). For batch processing the calculations of SS_χ and s, we wrote a collection of Perl scripts (available from the first author upon request).

Relationship between Average Squared Deviation s and Nodal Distance

Because the fossil cross-validation procedure might be influenced by the position of the calibration points relative to each other (Near et al., 2005a), we tested whether the average squared deviations s of the 72 calibration sets were correlated with the number of nodes separating the points of a calibration set (nodal distance; Fig. 2). For each calibration set, the total nodal distance was calculated by adding all pairwise nodal distances between each fixed calibration node and each of the five unconstrained nodes (step 1 of the fossil cross-validation; see above) and then summing up over all calibrations (step 4 of the fossil cross-validation). This calculation of total nodal distance thus reflects the goal of the present study; i.e., comparing the global internal consistencies among entire calibration sets (see Table 2). Correlation significance was tested by using the F-test statistic under a linear regression model in R (R Development Core Team, 2004). Because the 72 calibration sets differed in their degree of correlation between average squared deviation s and nodal distance (Fig. 2), we also calculated the percent deviation of s from the regression line with nodal distance for each calibration set (see Table 2) and plotted the results as a histogram (Fig. 3). The percent deviation of s represents a corrected measure of internal consistency among the calibration points of a set, termed "corrected calibration-set consistency" from now on.

Effect of Corrected Calibration-Set Consistency on Dating Precision

In order to check whether there is a relationship between the corrected calibration-set consistency and the precision of the dating estimates for the node of interest (node X; see Fig. 1), we plotted the percent standard deviation for the age of node X calculated for each of the 72 calibration sets (see below) against the percent deviation of s from the regression line with nodal distance (see Table 2; Fig. 4). Correlation significance was then tested with an F-test statistic under a linear regression model in R.

RESULTS

Phylogenetic Analyses

The data sets used for the phylogenetic analyses contained a total of 5124 aligned positions or characters (chars) for 74 taxa, comprising three plastid and two nuclear partitions: *rbc*L (1144 chars), *ndh*F (818 chars), *rpl*16-intron (560 chars), nr18S (1634 chars), and nr26S (968 chars; see online appendix at http://systematicbiology.org for GenBank accession numbers and TreeBASE study accession number S1775 for data matrix and tree definition). The optimal models of molecular evolution selected by MrAIC (Nylander, 2005b) were: SYM+I+G for *rbc*L, GTR+G for *ndh*F, GTR+G for *rpl*16-intron, SYM+I+G for nr18S, and GTR+I+G for nr26S. In all cases, the AICc and BIC criteria applied in MrAIC (Nylander, 2005b) selected the same models.

The MrBayes majority-rule consensus tree, including maximum likelihood branch lengths (optimized in *estbranches*), maximum likelihood bootstrap support values (estimated in BootPHYML 3.4), and Bayesian clade credibility values (calculated in MrBayes), is shown in Figure 1. The tree topology is congruent with published phylogenies (Conti et al., 2002; Renner, 2004;
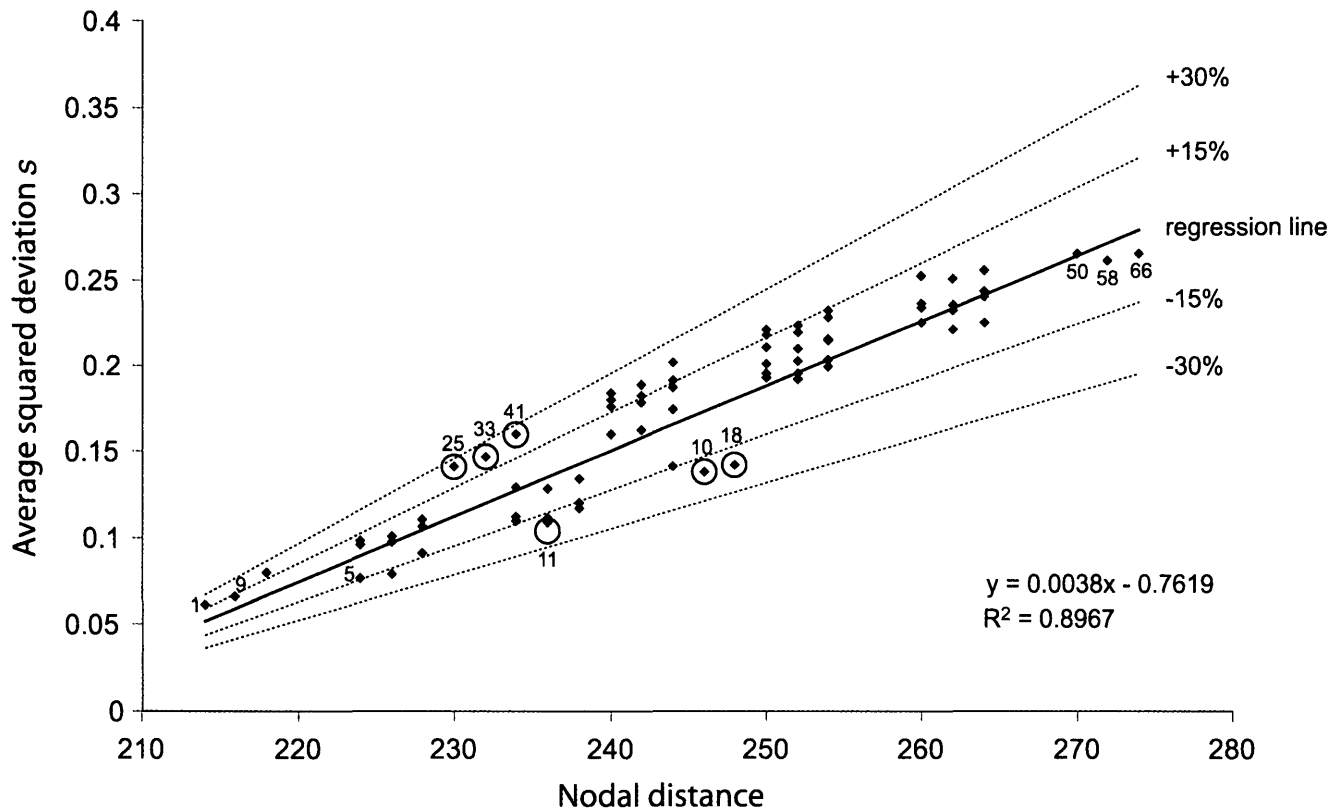
FIGURE 2. Correlation between the average squared deviation s and nodal distance among calibration points for each calibration set (see Table 2). R represents Pearson's correlation coefficient. Calibration sets 1, 9, 5 and 50, 66, 58 represent the sets with the lowest and highest s values, respectively. Calibration sets 18, 10, 11 and 33, 41, 25 (circled) show the s values that deviate the most below and above the regression line, respectively. The dotted lines above and below the regression line mark a deviation of $\pm15\%$ and $\pm30\%$ from the regression line, respectively.

Rutschmann et al., 2004; Schönenberger and Conti, 2004; Sytsma et al., 2004; Wilson et al., 2005). The well-supported Southeast Asian Crypteroniaceae are sister to a clade formed by the Central/South American Alzateaceae and the African Rhynchocalycaceae, Oliniaceae, and Penaeaceae. *Memecylon* is weakly supported as sister to Melastomataceae, corroborating the phylogenies of Clausing and Renner (2001) and Renner (2004). Within Melastomataceae, Melastomeae, Miconieae, and Merianieae are well supported as monophyletic. Within Myrtaceae s.l., Psiloxyloideae are sister to the rest of the clade, referred to as Myrtaceae s.s. (syn. Myrtoideae), in agreement with the phylogeny of Wilson et al. (2005). Myrteae, Melaleuceae, Eucalypteae, and Leptospermeae are all monophyletic, as in Wilson et al. (2005). The position of Vochysiaceae sister to Myrtaceae s.l. confirms the results of Sytsma et al. (2004) and Wilson et al. (2005). The relationships among the sampled Onagraceae are resolved as in Berry et al. (2004), Conti et al. (1993), and Levin et al. (2003).

Finding the Most Internally Consistent Calibration Sets by Using Fossil Cross-Validation

The five steps to calculate the average squared deviations (s values) were performed for all 72 calibration sets within 24 h by using two personal computers with 3-GHz Intel Pentium IV processors simultaneously. The s scores calculated in the fossil cross-validation analyses ranged from 0.061 (with calibration set 1) to 0.265 (with calibration sets 50 and 66; Table 2). The lowest s score was generated by the calibration set where all six fossils were assigned to stem nodes, whereas the highest s score was produced by a set with most fossils assigned to crown nodes (Table 2). The use of penalized likelihood (implemented in r8s) instead of Bayesian dating (implemented in *multidivtime*) to estimate divergence times did not affect the s scores substantially; i.e., the ranking of the s scores remained unchanged (data not shown).

Relationship between Average Squared Deviation s and Nodal Distance

The linear regression between the average squared deviations s of the 72 calibration sets and the distances in number of nodes between the calibration points of each calibration set produced an R^2 of 0.8967 (Fig. 2). The F-test statistic showed a significant correlation (degrees of freedom 1 and 70; $P < 2.2 \times 10^{-16}$). The three calibration sets with the lowest s values were 1, 9, and 5 (Fig. 2, left), while the three sets with the highest s values were 50, 58, and 66 (Fig. 2, right).

Twelve calibration sets had s values at least 10% lower than expected based on the regression line with nodal

TABLE 2. Characteristics of the 72 different calibration sets, each consisting of six calibration points: Average squared deviation s (see Fig. 2); nodal distances summed up over all fossil cross-validation steps (see Fig. 1); percent deviation of s from regression line with nodal distances (see Fig. 3); mean ages of node X (see Fig. 1) with percent standard deviations and 95% credibility intervals (see Fig. 4). The three sets with the highest level of corrected calibration-set consistency are shaded in light grey, whereas the three sets with the lowest corrected consistency are shaded in dark grey (see Fig. 3). Note that fossil 2 could be assigned to only one node in our phylogeny (node 2).

| Calibration set | Calibration points | | | | | | Average squared deviation s | Nodal distances | Percent deviation of s from regression line | Mean age of node X (My) | SD (in percent of mean age) | 95% Credibility interval | |
	1	2	3	4	5	6						2.5th percentile	97.5th percentile
1	a	2	a	a	a	a	0.0610	214	15.870	72.80	10.88	57.25	88.81
2	a	2	a	b	b	b	0.1411	244	−17.133	78.14	9.69	63.14	92.22
3	a	2	a	a	b	b	0.1098	234	−15.960	76.66	9.94	61.30	91.12
4	a	2	a	b	a	a	0.0982	224	9.053	75.83	10.20	60.72	91.06
5	a	2	a	a	a	b	0.0769	224	−16.133	74.40	10.59	59.24	89.71
6	a	2	a	b	b	a	0.1291	234	1.419	77.27	9.93	61.27	92.36
7	a	2	a	a	b	a	0.0957	224	6.689	74.80	10.39	59.17	89.99
8	a	2	a	b	a	b	0.1120	234	−13.642	77.15	9.66	62.66	91.82
9	a	2	b	a	a	a	0.0662	216	11.062	75.55	10.43	59.63	90.29
10	a	2	b	b	b	b	0.1375	246	−25.719	79.14	9.27	64.44	93.31
11	a	2	b	a	b	b	0.1088	236	−23.954	78.15	9.59	62.97	91.98
12	a	2	b	b	a	a	0.1008	226	3.864	77.12	9.86	61.73	91.73
13	a	2	b	a	a	b	0.0792	226	−22.426	76.61	9.84	61.60	91.34
14	a	2	b	b	b	a	0.1285	236	−4.954	78.38	9.77	63.06	92.81
15	a	2	b	a	b	a	0.0977	226	0.865	76.81	10.01	61.21	91.95
16	a	2	b	b	a	b	0.1116	236	−20.846	78.19	9.51	62.86	92.43
17	a	2	c	a	a	a	0.0794	218	16.299	77.08	10.12	61.21	91.72
18	a	2	c	b	b	b	0.1417	248	−27.351	79.70	9.48	64.47	94.76
19	a	2	c	a	b	b	0.1169	238	−21.903	79.21	9.47	63.69	93.02
20	a	2	c	b	a	a	0.1102	228	5.136	78.01	10.03	61.76	92.96
21	a	2	c	a	a	b	0.0914	228	−14.361	78.50	9.64	62.56	92.77
22	a	2	c	b	b	a	0.1337	238	−6.553	78.36	9.79	62.63	92.96
23	a	2	c	a	b	a	0.1068	228	2.161	78.43	10.13	62.98	93.42
24	a	2	c	b	a	b	0.1200	238	−18.753	79.42	9.60	63.76	93.87
25	b	2	a	a	a	a	0.1414	230	20.730	72.84	11.52	56.80	89.34
26	b	2	a	b	b	b	0.2246	260	−0.661	79.30	10.26	63.07	94.74
27	b	2	a	a	b	b	0.1925	250	2.265	76.61	10.99	60.31	93.44
28	b	2	a	b	a	a	0.1794	240	16.351	75.99	11.25	59.39	92.26
29	b	2	a	a	a	b	0.1596	240	5.926	74.55	11.78	58.50	92.04
30	b	2	a	b	b	a	0.2104	250	10.601	77.48	11.08	60.92	93.88
31	b	2	a	a	b	a	0.1762	240	14.793	74.64	11.50	58.15	91.25
32	b	2	a	b	a	b	0.1955	250	3.781	77.69	10.89	60.69	93.73
33	b	2	b	a	a	a	0.1468	232	18.448	74.92	11.78	58.32	92.23
34	b	2	b	b	b	b	0.2211	262	−5.682	79.76	10.52	63.48	95.23
35	b	2	b	a	b	b	0.1916	252	−2.128	78.40	11.01	60.82	94.68
36	b	2	b	b	a	a	0.1822	242	13.427	77.53	11.02	60.81	94.36
37	b	2	b	a	a	b	0.1619	242	2.608	76.98	11.19	60.23	93.92
38	b	2	b	b	b	a	0.2099	252	6.773	78.52	10.96	61.57	95.03
39	b	2	b	a	b	a	0.1783	242	11.562	76.20	11.28	59.39	93.04
40	b	2	b	b	a	b	0.1952	252	−0.248	78.79	10.71	62.39	94.58
41	b	2	c	a	a	a	0.1599	234	20.387	76.58	11.28	59.42	93.34
42	b	2	c	b	b	b	0.2252	264	−7.131	80.43	10.45	63.90	96.26
43	b	2	c	a	b	b	0.1996	254	−1.861	78.81	10.60	61.89	94.17
44	b	2	c	b	a	a	0.1914	244	13.646	78.27	10.97	61.70	95.00
45	b	2	c	a	a	b	0.1740	244	5.026	78.43	10.99	61.70	95.19
46	b	2	c	b	b	a	0.2150	254	5.450	79.21	10.81	62.70	95.82
47	b	2	c	a	b	a	0.1873	244	11.735	77.16	11.40	60.38	94.60
48	b	2	c	b	a	b	0.2035	254	0.089	79.84	10.02	63.51	95.53
49	c	2	a	a	a	a	0.1835	240	18.205	74.49	11.58	58.29	91.65
50	c	2	a	b	b	b	0.2654	270	0.502	79.54	11.12	62.21	96.80
51	c	2	a	a	b	b	0.2335	260	3.177	76.92	11.46	59.50	94.27
52	c	2	a	b	a	a	0.2213	250	14.999	77.40	11.42	59.56	94.04
53	c	2	a	a	a	b	0.2008	250	6.307	76.19	11.54	59.28	93.81
54	c	2	a	b	b	a	0.2521	260	10.316	78.20	11.17	61.17	95.89
55	c	2	a	a	b	a	0.2181	250	13.757	76.47	11.63	58.85	93.67
56	c	2	a	b	a	b	0.2365	260	4.380	78.17	11.08	61.25	94.98
57	c	2	b	a	a	a	0.1884	242	16.280	76.51	11.21	59.66	93.18
58	c	2	b	b	b	b	0.2614	272	−3.921	80.37	10.63	63.11	96.18
59	c	2	b	a	b	b	0.2322	262	−0.655	78.37	11.43	60.34	96.05
60	c	2	b	b	a	a	0.2235	252	12.441	78.92	10.91	61.62	95.37
61	c	2	b	a	a	b	0.2026	252	3.418	77.64	11.27	60.70	95.12
62	c	2	b	b	b	a	0.2511	262	6.936	79.43	10.97	62.31	96.32
63	c	2	b	a	b	a	0.2198	252	10.947	77.35	11.38	59.40	93.97
64	c	2	b	b	a	b	0.2357	262	0.839	79.77	10.95	62.06	96.74

(continued)

TABLE 2. Characteristics of the 72 different calibration sets, each consisting of six calibration points: Average squared deviation s (see Fig. 2); nodal distances summed up over all fossil cross-validation steps (see Fig. 1); percent deviation of s from regression line with nodal distances (see Fig. 3); mean ages of node X (see Fig. 1) with percent standard deviations and 95% credibility intervals (see Fig. 4). The three sets with the highest level of corrected calibration-set consistency are shaded in light grey, whereas the three sets with the lowest corrected consistency are shaded in dark grey (see Fig. 3). Note that fossil 2 could be assigned to only one node in our phylogeny (node 2).

	Calibration points						Average squared deviation s	Nodal distances	Percent deviation of s from regression line	Mean age of node X (My)	SD (in percent of mean age)	95% Credibility interval	
												2.5th percentile	97.5th percentile
Calibration set	1	2	3	4	5	6							
65	c	2	c	a	a	a	0.2013	244	17.890	77.80	11.16	59.91	94.11
66	c	2	c	b	b	b	0.2654	274	−5.245	81.46	10.67	64.39	98.24
67	c	2	c	a	b	b	0.2400	264	−0.554	79.74	10.69	63.31	96.77
68	c	2	c	b	a	a	0.2326	254	12.595	79.31	10.97	62.18	95.73
69	c	2	c	a	a	b	0.2146	254	5.256	79.12	11.25	61.32	95.80
70	c	2	c	b	b	a	0.2560	264	5.759	80.57	10.79	63.24	97.94
71	c	2	c	a	b	a	0.2285	254	11.047	78.48	11.22	61.27	95.67
72	c	2	c	b	a	b	0.2438	264	1.013	80.64	10.72	63.42	97.54

distance (termed "calibration sets A" from now on; see Fig. 3, left side). In all 12 sets, fossil 1 was always assigned to node 1a, and fossil 6 to node 6b, whereas the nodal assignments of fossils 3, 4, and 5 varied (Table 3). More specifically, calibration sets 18, 10, and 11 (Fig. 2) showed the s values that deviated the most below the regression line (−27.35%, −25.72%, and −23.95%, respectively; Table 2 and Fig. 3). Based on these results, we conclude that these three sets are characterized by the highest level of internal consistency corrected for nodal distance (corrected calibration-set consistency). Experiments of sequential removal of calibration points from each of calibration sets 18, 10, and 11, following the procedure by Near and Sanderson (2004), never produced a statistically significant decrease of the average squared deviation s between estimated and fossil ages (significance level set at $P = 0.01$; figure available online at http://systematicbiology.org), indicating that no calibration points should be removed from the most consistent calibration sets.

Twenty-three calibration sets were associated with s values that were at least 10% higher than expected from the regression line (Fig. 3, right side; named "calibration sets B" from now on). More specifically, calibration sets 33, 41, and 25 (Fig. 2) showed the s values that deviated the most above the regression line (18.45%; 20.39%; 20.73%, respectively; Table 2 and Figure 3). Based on these results, we conclude that these three calibration sets are characterized by the lowest level of internal consistency corrected for nodal distance (corrected calibration-set consistency).

Effect of Corrected Calibration-Set Consistency on Dating Precision

The correlation between the corrected measure of calibration-set consistency (defined as percent deviation of s from the regression line with nodal distance) and the percent standard deviation for the age of node X was significant (Fig. 4). Linear regression resulted in a multiple R^2 of 0.5975, and the F-test statistic showed a significant correlation (degrees of freedom 1 and 70; $P < 1.788$

$\times 10^{-16}$). The three calibration sets 18, 10, and 11 produced lower standard deviations for the age of node X than the three calibration sets 33, 41, and 25 (Table 2 and Fig. 4).

DISCUSSION

To our knowledge, this is the first study that explores the application of fossil cross-validation to the problem of nodal assignment for selected fossils. Although we realize that the results presented here by no means represent a panacea to the complex challenges of calibration (Magallón, 2004; Müller and Reisz, 2005; Near and Sanderson, 2004; Reisz and Müller, 2004; Wray, 2001), we nevertheless hope that our approach is useful when uncertainty exists on the placement of fossils to specific calibration nodes.

Despite well-founded theoretical guidelines (Doyle and Donoghue, 1993; Hennig, 1969; Magallón, 2004; Patterson, 1981; Sanderson, 1998), it is often difficult in practice to determine the exact phylogenetic placement of fossils on the basis of their morphological traits (Doyle and Donoghue, 1992; Manchester and Hermsen, 2000). The uncertainty of nodal assignment might be especially severe for the paleobotanical record, due to the generally lower degree of morphological integration in plants as compared to animals (Donoghue et al., 1989; Doyle and Donoghue, 1987, 1992; Hennig, 1966). Although exhaustive cladistic morphological analyses of extinct and extant taxa should allow for more reliable attachment of fossils to specific nodes, such analyses are rarely available (Donoghue et al., 1989; Doyle and Donoghue, 1993; Hermsen et al., 2003). In most cases, practitioners must depend on published descriptions of the morphological features of a fossil, which are often vague and contradictory when it comes to placing it in a phylogeny (Collinson and Pingen, 1992; Hickey, 1977; Manchester and Hermsen, 2000; Pigg et al., 1993; Rozefelds, 1996). Therefore, a careful review of the paleontological literature for a given group of taxa might lead to multiple nodal assignments of a selected fossil that can be equally defended on the basis of morphology.
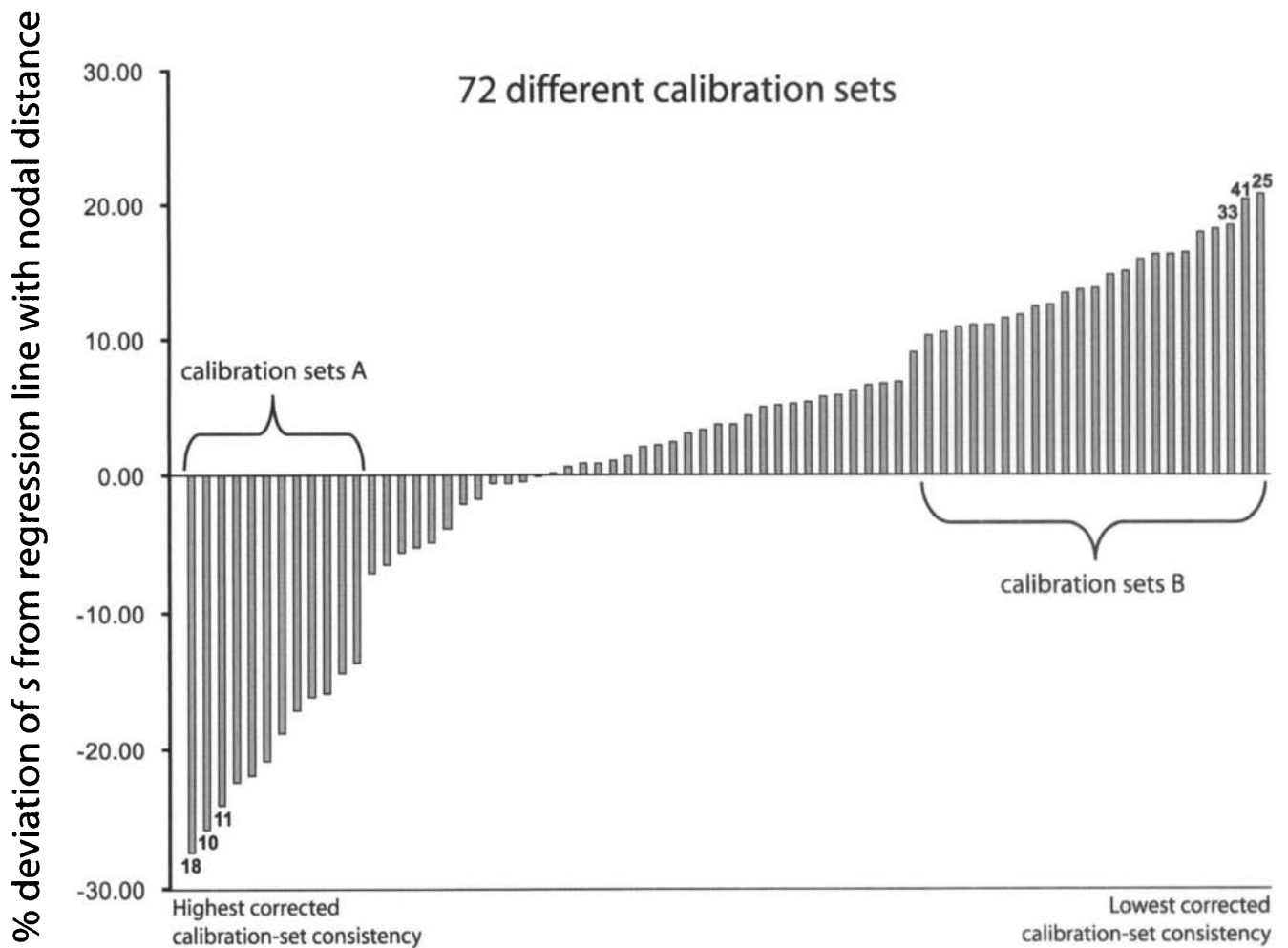
FIGURE 3. Histogram representing the percent deviation of s from the regression line of Figure 2 for all 72 calibration sets. Twelve calibration sets showed s values that were at least 10% lower than expected from the regression line (calibration sets A). These sets are associated with the highest level of corrected calibration-set consistency. Twenty-three calibration sets showed s values that were at least 10% higher than expected from the regression line (calibration sets B). These sets are associated with the lowest level of corrected calibration-set consistency.

The possibility of attaching fossils to multiple nodes also depends on the density of taxon sampling in the relevant phylogenetic neighborhood. In many dated chronograms, only one possible assignment exists, because only one taxon was sampled from the pertinent group (e.g., the assignment of fossil Melastomataceae leaves in Conti et al., 2002, or the assignment of fossil Eucalyptoid fruits in Sytsma et al., 2004; see also Sanderson and Doyle, 2001). Although unequivocal, this procedure is hardly satisfactory. In the study presented here, we designed taxon sampling in order to allow for multiple nodal assignment possibilities. In fact, five out of the six selected Myrtales fossils (Table 1) could be justifiably assigned to more than one node, based on the morphological traits discussed in the paleobotanical literature (Collinson and Pingen, 1992; Hickey, 1977; Pigg et al., 1993; Rozefelds, 1996). In total, 72 different assignment combinations (calibration sets) were possible, each comprising six calibration points (Table 2).

Finding the Most Internally Consistent Calibration Sets by Using Fossil Cross-validation

In this study of Crypteroniaceae and related taxa, we use the fossil cross-validation procedure of Near and Sanderson (2004) in a novel way to assess uncertainty in fossil nodal assignment. More specifically, our goal is to identify the most congruent calibration sets by comparing the internal consistencies of all 72 calibration sets generated from alternative placements of six fossils (Table 2). Our procedure differs from that described by Near and Sanderson (2004) in one important respect. Their original implementation of fossil cross-validation relied on $SS\chi$ values (i.e., sums of squared differences between fossil and estimated molecular ages) that were calculated based on a single calibration point (see steps 1 to 3 in Materials and Methods). The $SS\chi$ values then guided the removal of selected fossils that were in conflict with the other fossils of a multiple calibration set. Therefore, the $SS\chi$ values utilized for fossil removal were influenced by
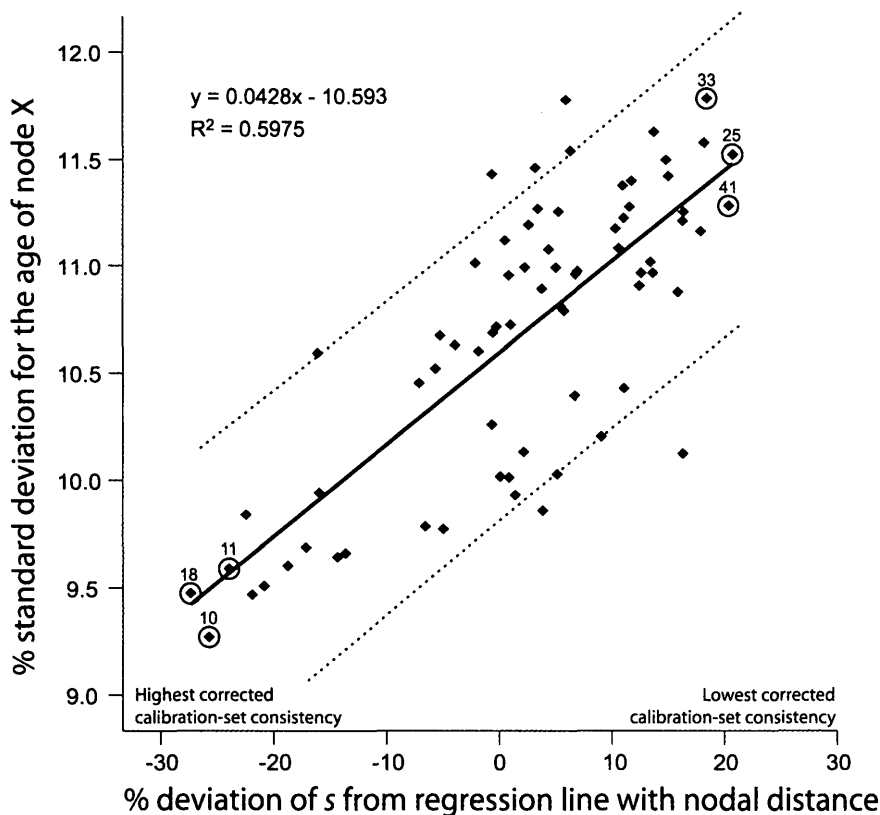
FIGURE 4.   Correlation between corrected calibration-set consistency (expressed as percent deviation of s from the regression line with nodal distance; see Figs. 2 and 3) and percent standard deviation for the age of node X. The three calibration sets 18, 10, and 11 produced lower standard deviations for the age of node X than the three calibration sets 33, 41, and 25. The dotted lines above and below the regression line represent the 95% prediction interval, the area in which 95% of all data points are expected to fall.

the idiosyncrasies of the single calibration points used in their calculation. Conversely, in our implementation of fossil cross-validation, we calculate the average squared deviation s for an entire calibration set by using all six fossils as calibration points (see steps 4 to 5 in Materials and Methods). We then employ these average s values to compare the internal consistencies of all 72 calibration sets, each one including all six fossils. Therefore, our procedure is less influenced by the peculiarities of individual deviations between the age of the fossil used for calibration during fossil cross-validation and the actual age of nodal divergence for the same calibration point.

The analyses revealed large differences among the average squared deviations associated with the 72 calibration sets, ranging from an s value of 0.061 for set 1 to an s value of 0.265 for set 66 (Table 2; Fig. 2). Therefore, one might conclude that the assignment of fossils 1, 2, 3, 4, 5, and 6 to nodes $1a$, 2, $3a$, $4a$, $5a$, and $6a$, respectively, produced the most internally consistent calibration set, while the assignment of the same fossils to nodes $1c$, 2, $3c$, $4b$, $5b$, and $6b$, respectively, produced the most inconsistent one. However, in calibration set 1 all the fossils are assigned to their stem nodes, while in calibration set 66 all the fossils are assigned to their crown nodes, except for fossil 2, for which only one nodal assignment is pos-

sible (Table 2). It is thus reasonable to ask whether the s values might be influenced by the nodal distance among calibration points. Indeed, a significant positive correlation between the average squared deviation s and nodal distances was observed for the calibration sets (Fig. 2).

How can we explain the correlation between s values and nodal distance found in our study? It is important to remember that the s values are essentially derived from the difference between the estimated and the fossil ages of the calibration points in a set. Therefore, one possible interpretation of the observed correlation might

TABLE 3.   Distribution of calibration points in calibration sets A (see Fig. 3). The letter x in the "consensus" set indicates that, among the 12 calibration sets, the fossil was assigned to all possible calibration nodes.

| Fossil | Nodal assignments in the 12 calibration sets A | | |
	a	b	c
1	All 12	0	0
2	—	—	—
3	4	4	4
4	6	6	—
5	6	6	—
6	0	All 12	—
Consensus:	$1a$ 2 $3x$ $4x$ $5x$ $6b$		

relate to the procedures used for nodal age estimation. More specifically, the rate smoothing methods employed in our dating analyses, based on both Bayesian (Thorne et al., 1998) and penalized likelihood (Sanderson, 2002) approaches, allow rates to change between ancestral-descendant branches, thus creating estimation errors that depend on the number of nodes involved in the smoothing procedure. Consequently, the greater the nodal distance among calibration points, the greater the possible difference between the estimated and the fossil ages of the calibration points in a set. Because greater nodal distances are associated with sets where fossils are mostly assigned to the corresponding crown nodes (see Fig. 1 and Table 2), this would explain why such sets are characterized by greater s values, as in the case of set 66 (Fig. 2). Conversely, calibration sets where most fossils are attached to the stem nodes, as in the case of set 1, are associated with smaller nodal distances among calibration points, hence with smaller s values (Fig. 2; Table 2). Thus, our results suggest that the smaller s values associated with calibration sets where most fossils are assigned to stem nodes do not inherently reflect a higher level of consistency among the calibration points, but the effects of nodal distance. Therefore, s values appear to represent a biased estimate of internal consistency.

In order to identify the calibration sets least and most affected by nodal distance bias, we ranked all sets according to the percent deviation of s from the regression line with nodal distance (Fig. 3). This allowed us to recognize calibrations sets 18, 10, and 11 as those associated with the highest level of internal consistency corrected for nodal distance, and sets 33, 41, and 25 as those with the lowest level of corrected internal consistency (Table 2). Importantly, the most consistent calibration sets also produced the lowest percent standard deviations for the estimated ages of node X and the least consistent sets the highest percent standard deviations (Fig. 4). This positive correlation might be explained by the observation that inconsistent calibration points in a set contradict each other in their statements about the timing of evolutionary events, thus producing conflicting estimates for the age(s) of the node(s) of interest, hence higher associated errors (Near and Sanderson, 2004; Near et al., 2005b). Conversely, calibration points in sets with high levels of corrected internal consistency produce convergent estimates for the age(s) of the node(s) of interest, hence lower associated errors.

The 12 calibration sets associated with the highest level of corrected internal consistency (Fig. 3, left side) share some common properties. In all, the temporal information provided by fossil 1 is most consistent with that of the other calibration points if it is assigned to node 1*a* (Table 3 and Fig. 1). This result supports the interpretation by Renner et al. (2001) and Sytsma et al. (2004) that the fossil leaves from the Early Eocene of North Dakota (Hickey, 1977) should be assigned to the node representing the entire Melastomataceae crown group, because of the acrodromous leaf venation. On the other hand, fossil 6, representing the pollen *Diporites aspis* from the Early Oligocene of Otway Basin (Australia; Berry et al.,

1990; Table 1), is most consistent with the other calibration points if it is assigned to node 6*b*, representing the *Fuchsia* crown group (Table 3 and Fig. 1). This conclusion is congruent with the results of molecular dating analyses that produced an age interval for the node corresponding to 6*b* compatible with the age of *Diporites aspis* (Berry et al., 2004; Sytsma et al., 2004).

No clear pattern emerges from comparisons among calibration sets A for the assignment of fossils 3, 4, and 5 (Table 3). However, in the calibration set with the highest level of corrected internal consistency (18; Table 2 and Fig. 5), the three fossils are all assigned to their crown positions (nodes 3*c*, 4*b*, and 5*b*; Fig. 1). Based on this evidence, the pollen *Myrtaceidites lisamae* from the Santonian of Gabon (fossil 3) is most consistently attributed to Myrtaceae s.s. (node 3*c*), as proposed by Sytsma et al. (2004). Also in agreement with Sytsma et al. (2004), the fruits and seeds of *Paleomyrtinaea* from the latest Paleocene of North Dakota (fossil 4) are most consistently placed with the crown radiation of the tribe Myrteae (Myrtoideae s.s.; node 4*b*). Finally, the Eucalypt-like fruits from the Middle Eocene of South Eastern Queensland (fossil 5) are best assigned to the node representing the most recent common ancestor of *Eucalyptus* and *Angophora* (node 5*b*), as suggested by Rozefelds (1996).

In the calibration set with the highest level of corrected internal consistency (18; Table 2 and Fig. 5), four out of the six fossils are attributed to the crown nodes of the relevant clades (*3c, 4b, 5b, 6b*) and only one to the stem node (*1a*; Fig. 1). Because fossils represent extinct members of either crown or stem groups (Magallon, 2004), it is not surprising that different fossils in an optimal multicalibration set may be attached to different positions. Despite the seeming simplicity of the conceptual distinction between stem and crown assignments, the actual decision of attaching individual fossils to either the stem or crown node is indeed very complex, because it would require detailed knowledge about the distribution of synapomorphies among extinct and extant taxa (Magallón, 2004). Unfortunately, the comprehensive cladistic morphological analyses necessary to achieve a sound attribution of fossils to the proper nodes is usually unavailable (Conti et al., 2004; Magallon, 2004; Near et al., 2005b). Our study thus represents an alternative approach to the difficult decision of fossil nodal assignment.

The Age of Node X and the Biogeographic Origin of Crypteroniaceae

All estimates generated in this study (Table 2) for the mean age of the split between the Southeast Asian Crypteroniaceae and their West Gondwanan sister clade are contained within the interval ranging from 81.5 to 72.8 My. The age estimate derived from the calibration set with the highest level of corrected calibration-set consistency (18) is comprised between 72.15 and 87.25 My (Fig. 5). These results are both compatible with and more precise than published age estimates for the same node (106 to 141 My, Conti et al., 2002; 62 to 109 My, Rutschmann et al., 2004). However, it is important to note that the
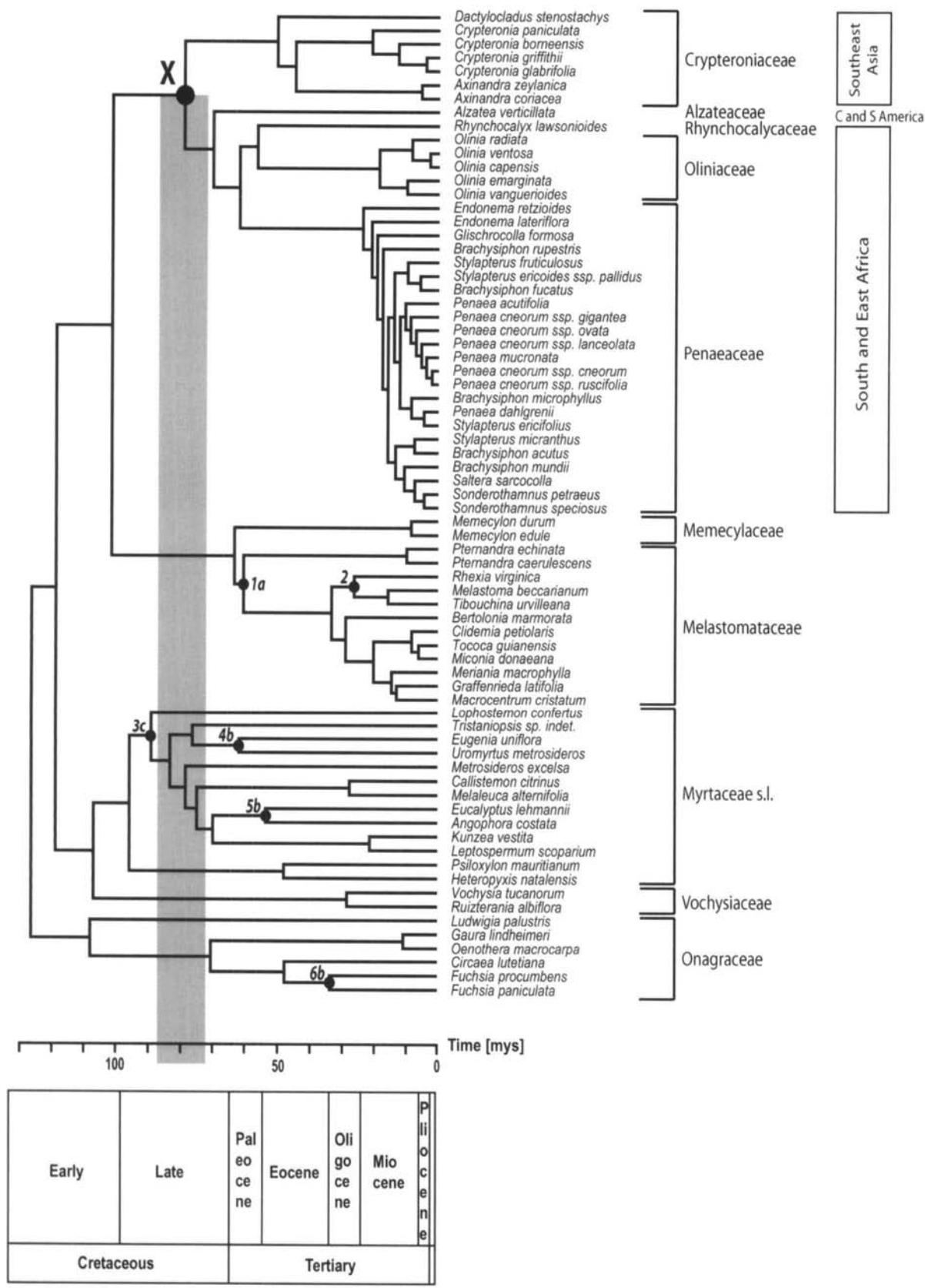
FIGURE 5.   The chronogram derived from the calibration set with the highest level of corrected calibration-set consistency (18; see Table 2). The corresponding calibration points (*1a, 2, 3c, 4b, 5b, 6b*) are marked on the tree.

mentioned studies differed from the one presented here both in gene/taxon sampling and calibration strategies. Despite these differences in the precision of the age estimates, the biogeographic scenario most congruent with the timeframes calculated for node X is that the Crypteroniaceae stem lineage dispersed from Africa to the Deccan plate as the latter drifted northward in relative proximity to the African coast during the Late Cretaceous (approximately 125 to 84 Mya; McLoughlin, 2001; Plummer and Belle, 1995). The newly obtained age estimates, then, further support India's likely role in expanding the range of Crypteroniaceae from Africa to Asia during its northbound movement along the African coast, corroborating the out-of-India hypothesis for the origin of Crypteroniaceae (Conti et al., 2002, 2004; Moyle, 2004; Rutschmann et al., 2004; see also Lieberman, 2003).

CONCLUSIONS

To summarize, our study illustrates a novel approach to the problem of nodal fossil assignment when equally justifiable alternatives exist. It uses an expanded fossil cross-validation procedure to identify the calibration sets with the highest level of internal consistency. After correcting for nodal distance bias, these sets can be used to estimate the ages of the nodes of interest. An important outcome of our study is that the calibration sets with the higher corrected internal consistency produced lower standard deviations associated with nodal age estimates than sets characterized by lower levels of corrected consistency. The improved precision of the estimate is a desirable property of any analytical tool.

Although we have attempted to suggest a practical approach, based on a modified implementation of available methodology (i.e., fossil cross-validation; Near and Sanderson, 2004; Near et al., 2005b), to address the fundamental, yet under-studied problem of uncertainty in fossil nodal assignment, we also wish to emphasize that such measures can by no means replace careful review, selection, and evaluation of the fossil record used for calibration. To further improve the procedure of fossil calibration, a multi-pronged approach will be necessary, including comprehensive morphological cladistic analyses of extinct and extant taxa (Donoghue et al., 1989; Doyle, 2000; Eklund et al., 2004), estimation of the gap between the time of lineage divergence and the time of first appearance of synapomorphies in the fossil record (Foote and Sepkoski, 1999; Tavaré et al., 2002), improved paleontological dating of fossils, and evaluation of the positional effects of calibration nodes in relation to the nodes of interest (Conroy and van Tuinen, 2003; Porter et al., 2005; Smith and Peterson, 2002). Ultimately, the development of methods that incorporate a priori all sources of fossil calibration uncertainty in the procedure of nodal age estimation would represent a real advancement towards addressing one of the thorniest problems of molecular dating and improving the accuracy of the estimated ages.

REFERENCES

Alroy, J. 1999. The fossil record of North American mammals: Evidence for a Paleocene evolutionary radiation. Syst. Biol. 48:107–118.

Anderson, J. A. R., and J. Muller. 1975. Palynological study of a Holocene peat and a Miocene coal deposit from NW Borneo. Rev. Palaeobot. Palynol. 19:291–351.

Aris-Brosou, S., and Z. Yang. 2002. Effects of models of rate evolution on estimation of divergence dates with special reference to the metazoan 18S ribosomal RNA phylogeny. Syst. Biol. 51:703–714.

Ashton, P. S., and C. V. S. Gunatilleke. 1987. New light on the plant geography of Ceylon: I. Historical plant geography. J. Biogeogr. 14:249–285.

Baum, D. A., R. L. Small, and J. F. Wendel. 1998. Biogeography and floral evolution of baobabs (*Adansonia*, Bombacaceae) as inferred from multiple data sets. Syst. Biol. 47:181–207.

Bell, C. D., and M. J. Donoghue. 2005. Dating the Dipsacales: Comparing models, genes, and evolutionary implications. Am. J. Bot. 92:284–296.

Benton, M. J., and F. J. Ayala. 2003. Dating the tree of life. Science 300:1698–1700.

Berry, P. E., W. J. Hahn, K. J. Sytsma, J. C. Hall, and A. Mast. 2004. Phylogenetic relationships and biogeography of *Fuchsia* (Onagraceae) based on noncoding nuclear and chloroplast DNA data. Am. J. Bot. 94:601–614.

Berry, P. E., J. J. Skvarla, A. D. Partridge, and M. K. Macphail. 1990. *Fuchsia* pollen from the Tertiary of Australia. Aust. Syst. Bot. 3:739–744.

Boltenhagen, E. 1976. Pollens et spores Sénoniennes du Gabon. Cahiers de Micropaléontologie 17:1–21.

Bossuyt, F., and M. C. Milinkovitch. 2001. Amphibians as indicators of early Tertiary "out-of-India" dispersal of vertebrates. Science 292:93–95.

Brochu, C. A. 2004. Calibration age and quartet divergence date estimation. Evolution 58:1375–1382.

Bult, C., M. Källersjö, and Y. Suh. 1992. Amplification and sequencing of 16/18S rDNA from gel-purified total plant DNA. Plant Mol. Biol. Rep. 10:273–284.

Christophel, D. C., L. J. Scriven, and D. R. Greenwood. 1992. An Eocene megafossil flora from Nelly Creek, South Australia. Trans. R. Soc. S. Aust. 116:65–76.

Clausing, G., and S. S. Renner. 2001. Molecular phylogenetics of Melastomataceae and Memecylaceae: implications for character evolution. Am. J. Bot. 88:486–498.

Collinson, M. E., and M. Pingen. 1992. Seeds of the Melastomataceae from the Miocene of Central Europe. Pages 129–139 *in* Palaeovegetational development in Europe (J. Kovar-Eder, ed.) Museum of Natural History, Vienna, Austria.

Conroy, C. J., and M. van Tuinen. 2003. Extracting time from phylogenies: Positive interplay between fossil and genetic data. J. Mammal. 84:444–455.

Conti, E., T. Eriksson, J. Schönenberger, K. J. Sytsma, and D. A. Baum. 2002. Early Tertiary out-of-India dispersal of Crypteroniaceae: Evidence from phylogeny and molecular dating. Evolution 56:1931–1942.

Conti, E., A. Fischbach, and K. J. Sytsma. 1993. Tribal relationships in Onagraceae: Implications from *rbcL* sequence data. Ann. Missouri Bot. Gard. 80:672–685.

Conti, E., A. Litt, and K. J. Sytsma. 1996. Circumscription of Myrtales and their relationships to other Rosids: Evidence from *rbc*L sequence data. Am. J. Bot. 83:221–233.

Conti, E., A. Litt, P. G. Wilson, S. A. Graham, B. G. Briggs, L. A. S. Johnson, and K. J. Sytsma. 1997. Interfamilial relationships in Myrtales: Molecular phylogeny and patterns of morphological evolution. Syst. Bot. 22:629–647.

Conti, E., F. Rutschmann, T. Eriksson, K. J. Sytsma, and D. A. Baum. 2004. Calibration of molecular clocks and the biogeographic history of Crypteroniaceae: A reply to Moyle. Evolution 58:1874–1876.

Cowles, M. K., and B. P. Carlin. 1996. Markov chain Monte Carlo convergence diagnosis: A comparative review. J. Am. Stat. Assoc. 91:883–904.

Crane, P. R., S. R. Manchester, and D. L. Dilcher. 1990. A preliminary survey of fossil leaves and well-preserved reproductive stuctures from the Sentinel Butte Formation (Paleocene) near Almont, North Dakota. Fieldiana Geol. 1418:1–63.

Daghlian, C. P., J. J. Skvarla, D. T. Pocknall, and P. H. Raven. 1985. *Fuchsia* pollen from the early Miocene of New Zealand. Am. J. Bot. 72:1039–1047.

Dahlgren, R., and R. F. Thorne. 1984. The order Myrtales: Circumscription, variation, and relationships. Ann. Missouri Bot. Gard. 71:633–699.

Dahlgren, R., and A. E. Van Wyk. 1988. Structures and relationships of families endemic to or centered in Southern Africa. Monogr. Syst. Bot. Mo. Bot. Gard. 25:1–94.

Darwin, C. 1859. On the origin of species by means of natural selection or the preservation of favoured races in the struggle for life. John Murray, London.

de Queiroz, K., and J. Gauthier. 1990. Phylogeny as a central principle in taxonomy: Phylogenetic definitions of taxon names. Syst. Zool. 39:307–322.

Donoghue, M. J., J. A. Doyle, J. Gauthier, A. G. Kluge, and T. Rowe. 1989. The importance of fossils in phylogeny reconstruction. Ann. Rev. Ecol. Syst. 20:431–460.

Dorofeev, P. I. 1960. On the Tertiary flora of Belorussia. Botanichesky Zhurnal SSSR 45:1418–1434 (in Russian).

Dorofeev, P. I. 1963. The Tertiary floras of western Siberia. Izdatelstvo Akademii Nauk SSSR. Moskva-Leningrad, Russia (in Russian).

Dorofeev, P. I. 1988. Miocene floras of the Tambov district. Akademii Nauk, Leningrad, Russia (in Russian, posthumous work, F. Y. Velichkevich, ed.).

Doyle, J. A. 2000. Paleobotany, relationships, and geographic history of Winteraceae. Ann. Missouri Bot. Gard. 87:303–316.

Doyle, J. A., and M. J. Donoghue. 1987. The importance of fossils in elucidating seed plant phylogeny and macroevolution. Rev. Palaeobot. Palynol. 50:63–95.

Doyle, J. A., and M. J. Donoghue. 1992. Fossils and seed plant phylogeny reanalyzed. Brittonia 44:89–106.

Doyle, J. A., and M. J. Donoghue. 1993. Phylogenies and angiosperm diversification. Paleobiology 19:141–167.

Drummond, A. J., S. Y. W. Ho, M. J. Phillips, and A. Rambaut. 2006. Relaxed phylogenetics and dating with confidence. PLoS Biol. 4:e88.

Dyjor, S., Z. Kvacek, M. Lanucka-Srodoniowa, W. Pyszynski, A. Sadowska, and E. Zastawniak. 1992. The Younger Tertiary deposits in the Gozdnica region (SW Poland) in the light of recent palaeobotanical research. Pol. Bot. Stud. 3:1–129.

Eklund, H., J. A. Doyle, and P. S. Herendeen. 2004. Morphological phylogenetic analysis of living and fossil Chloranthaceae. Int. J. Plant Sci. 165:107–151.

Fairon-Demaret, M. 1994 [1996]. Les fruits et graines du Miocene de Bioul (Entre-Samre-et-Meuse, Belgique). Etude qualitative, quantitative et considerations paleoécologiques. Ann. Soc. Geol. Belgique 117:277–309.

Felsenstein, J. 2004. PHYLIP (phylogeny inference package), version 3.63. Department of Genetics, University of Washington, Seattle, Washington.

Foote, M., J. P. Hunter, C. M. Janis, and J. J. Sepkoski Jr. 1999. Evolutionary and preservational constraints on origins of biologic groups: Divergence times of Eutherian mammals. Science 283:1310–1314.

Foote, M., and J. J. Sepkoski Jr. 1999. Absolute measures of the completeness of the fossil record. Nature 398:415–417.

Graham, S. A. 1984. Alzateaceae, a new family of Myrtales in the American Tropics. Ann. Missouri Bot. Gard. 71:757–779.

Graur, D., and W. Martin. 2004. Reading the entrails of chickens: Molecular timescales of evolution and the illusion of precision. Trends Genet. 20:80–86.

Guindon, S., and O. Gascuel. 2003. A simple, fast, and accurate algorithm to estimate large phylogenies by maximum likelihood. Syst. Biol. 52:696–704.

Hedges, S. B., and S. Kumar. 2003. Genomic clocks and evolutionary timescales. Trends Genet. 19:200–206.

Hennig, W. 1966. Phylogenetic systematics. University of Illinois Press, Urbana, Illinois.

Hennig, W. 1969. Die Stammesgeschichte der Insekten. Kramer, Frankfurt, Germany.

Hermsen, E. J., M. A. Gandolfo, K. C. Nixon, and W. L. Crepet. 2003. *Divisestylus* gen. nov. (aff. Iteaceae), a fossil saxifrage from the Late Cretaceous of New Jersey, USA. Am. J. Bot. 90:1373–1388.

Herngreen, G. F. W. 1975. An Upper Senonian pollen assemblage of borehole 3-PIA-10-AL, State of Alagoas, Brazil. Pollen Spores 17:93–140.

Hickey, L. J. 1977. Stratigraphy and paleobotany of the Golden Valley formation (Early Tertiary) of western North Dakota. Memoir 150. Geological Society of America, Boulder, Colorado.

Ho, S. Y. W., and G. Larson. 2006. Molecular clocks: When the times are a-changin'. Trends Genet. 22:79–83.

Huelsenbeck, J. P., and F. Ronquist. 2001. MrBayes: Bayesian inference of phylogeny. Bioinformatics 17:754.

Johnson, L. A. S., and B. G. Briggs. 1984. Myrtales and Myrtaceae—A phylogenetic analysis. Ann. Missouri Bot. Gard. 71:700–756.

Kishino, H., J. L. Thorne, and W. J. Bruno. 2001. Performance of a divergence time estimation method under a probabilistic model of rate evolution. Mol. Biol. Evol. 18:352–361.

Kuzoff, R. K., J. A. Sweere, D. E. Soltis, P. S. Soltis, and E. A. Zimmer. 1998. The phylogenetic potential of entire 26S rDNA sequences in plants. Mol. Biol. Evol. 15:251–263.

Langley, C. H., and W. Fitch. 1974. An estimation of the constancy of the rate of molecular evolution. J. Mol. Evol. 3:161–177.

Lantern, L. R., and W. P. Sharp. 1989. Seed coat characters of some American Myrtinae (Myrtaceae): *Psidium* and related genera. Syst. Bot. 14:370–376.

Lantern, L. R., and D. Stevenson. 1986. Variability of embryos in subtribe Myrtinae (Myrtaceae). Syst. Bot. 11:155–162.

Lee, M. S. Y. 1999. Molecular clock calibrations and Metazoan divergence dates. J. Mol. Evol. 49:385–391.

Levin, R. A., W. L. Wagner, P. C. Hoch, M. Nepokroff, J. C. Pires, E. A. Zimmer, and K. J. Sytsma. 2003. Family-level relationships of Onagraceae based on chloroplast *rbc*L and *ndh*F data. Am. J. Bot. 90:107–115.

Lieberman, B. S. 2003. Unifying theory and methodology in biogegraphy. J. Evol. Biol. 33:1–25.

Macey, J. R., J. A. Schulte II, A. Larson, N. B. Ananjeva, Y. Wang, R. Rethiyagoda, N. Rastegar-Pouyani, and T. J. Papenfuss. 2000. Evaluating trans-Tethys migration: An example using acrodont lizard phylogenetics. Syst. Biol. 49:233–256.

Maddison, P. G., and D. R. Maddison. 2000. MacClade 4: Analysis of phylogeny and character evolution, version 4.0. Sinauer Associates, Sunderland, Massachusetts.

Magallón, S. A. 2004. Dating lineages: Molecular and paleontological approaches to the temporal framework of clades. Int. J. Plant Sci. 165:7–21.

Magallón, S. A., and M. J. Sanderson. 2001. Absolute diversification rates in Angiosperm clades. Evolution 55:1762–1780.

Magallón, S. A., and M. J. Sanderson. 2005. Angiosperm divergence times: The effect of genes, codon positions, and time constraints. Evolution 59:1653–1670.

Mai, D. H. 1995. Tertiäre Vegetationsgeschichte Europas. G. Fischer, Jena, Germany.

Mai, D. H. 2000. Die untermiozänen Floren aus der Spremberger Folge und dem II. Flözhorizont der Lausitz. Teil III. Dialypetalae und Sympetalae. Palaeontographica B 253:1–106.

Manchester, S. R. 1999. Biogeographical relationships of North American Tertiary floras. Ann. Missouri Bot. Gard. 86:472–522.

Manchester, S. R., and E. J. Hermsen. 2000. Flowers, fruits, seeds, and pollen of *Landeenia* gen. Nov., an extinct sapindalean genus from the Eocene of Wyoming. Am. J. Bot. 87:1909–1914.

Marshall, C. R. 1990a. Confidence intervals on stratigraphic ranges. Paleobiology 16:1–10.

Marshall, C. R. 1990b. The fossil record and estimating divergence times between lineages—Maximum divergence times and the importance of relieable phylogenies. J. Mol. Evol. 30:400–408.

McKenna, M. C. C. 1973. Sweepstakes, filters, corridors, Noah's arks, and beached Viking funeral ships in paleogeography. Pages 291–304 *in* Implications of continental drift to the earth sciences (D. H. Tarling, and S. K. Runcorn, eds.). Academic Press, London.

McLaughlin, S. 2001. The breakup history of Gondwana and its impact on pre-Cenozoic floristic provincialism. Aust. J. Bot. 48:271–300.

Mentink, H., and P. Baas. 1992. Leaf anatomy of the Melastomataceae, Memecylaceae, and Crypteroniaceae. Blumea 37:189–225.

Morley, R. J. 2000. Origin and evolution of tropical rain forests, 1st edition. John Wiley & Sons, Chichester, England.

Morley, R. J., and C. W. Dick. 2003. Missing fossils, molecular clocks and the origin of the Melastomataceae. Am. J. Bot. 90:1638–1645.

Moyle, R. G. 2004. Calibration of molecular clocks and the biogeographic history of Crypteroniaceae. Evolution 58:1871–1873.

Muller, J. 1968. Palynology of the Pedawan and Plateau Sandstone Formations (Creataceous-Eocene) in Sarawak, Malaysia. Micropaleontology 14:1–37.

Muller, J. 1975. Note on the pollen morphology of Crypteroniaceae s. l. . Blumea 22:275–294.

Muller, J. 1981. Fossil pollen records of extant angiosperms. Bot. Rev. 47:1–142.

Müller, J., and R. R. Reisz. 2005. Four well-constrained calibration points from the vertebrate fossil record for molecular clock estimates. BioEssays 27:1069–1075.

Near, T. J., D. I. Bolnick, and P. C. Wainwright. 2005a. Fossil calibrations and molecular divergence time estimates in centrarchid fishes (Teleostei: Centrarchidae). Evolution 59:1768–1782.

Near, T. J., P. A. Meylan, and H. B. Shaffer. 2005b. Assessing concordance of fossil calibration points in molecular clock studies: An example using turtles. Am. Nat. 165:137–146.

Near, T. J., and M. J. Sanderson. 2004. Assessing the quality of molecular divergence time estimates by fossil calibrations and fossil-based model selection. Philos. Trans. R. Soc. Lond. B Biol. Sci. 359:1477–1483.

Nylander, J. 2005a. BootPHYML 3.4. School of Computational Science (SCS), Florida State University, Tallahassee, Florida.

Nylander, J. 2005b. MrAIC 1.4. School of Computational Science (SCS), Florida State University, Tallahassee, Florida.

Olmstead, R. G., and J. A. Sweere. 1994. Combining data in phylogenetic systematics: An empirical approach using three molecular data sets in the Solanaceae. Syst. Biol. 43:467–481.

Patterson, C. 1981. Significance of fossils in determining evolutionary relationships. Ann. Rev. Ecol. Syst. 12:195–223.

Penny, D. 2005. Relativity for molecular clocks. Nature 436:183–184.

Pereira, J. T. 1996. Crypteroniaceae. Pages 135–149 *in* Tree flora of Sabah and Sarawak, volume 2 (E. Soepadmo, K. M. Wong, and L. G. Saw, eds.). Forest Research Institute Malaysia, Sabah Forestry Department, and Sarawak Forestry Department, Kuala Lumpur, Malaysia.

Pereira, J. T., and K. M. Wong. 1995. Three new species of *Crypteronia* (Crypteroniaceae) from Borneo. Sandakania 6:41–53.

Pigg, K. B., R. A. Stockey, and S. L. Maxwell. 1993. *Paleomyrtinaea*, a new genus of permineralized myrtaceous fruits and seeds from the Eocene of British Columbia and Paleocene of North Dakota. Can. J. Bot. 71:1–9.

Plummer, P. S., and E. R. Belle. 1995. Mesozoic tectono-stratigraphic evolution of the Seychelles microcontinent. Sediment. Geol. 96:73–91.

Porter, M. L., M. Pérez-Losada, and K. A. Crandall. 2005. Model-based multi-locus estimation of decapod phylogeny and divergence times. Mol. Phylogenet. Evol. 37:355–369.

Pulquério, M. J. F., and R. A. Nichols. 2007. Dates from the molecular clock: How wrong can we be? Trends Ecol. Evol. 22:180–184.

R Development Core Team. 2004. R: A language and environment for statistical computing. R Foundation for Statistical Computing, Vienna, Austria. Available from http://www.R-project.org.

Rambaut, A., and A. J. Drummond. 2005. Tracer 1.3. A program for analyzing results from Bayesian MCMC programs such as BEAST & MrBayes. Department of Zoology, University of Oxford, Oxford, UK. Available from http://evolve.zoo.ox.ac.uk/software.html.

Reisz, R. R., and J. Müller. 2004. Molecular timescales and the fossil record: a paleontological perspective. Trends Genet. 20:237–241.

Renner, S. S. 2004. Bayesian analysis of combined chloroplast loci, using multiple calibrations, supports the recent arrival of Melastomataceae in Africa and Madagascar. Am. J. Bot. 91:1427–1435.

Renner, S. S. 2005. Relaxed molecular clocks for dating historical plant dispersal events. Trends Plant Sci. 10:550–558.

Renner, S. S., G. Clausing, and K. Meyer. 2001. Historical biogeography of Melastomataceae: The roles of Tertiary migration and long-distance dispersal. Am. J. Bot. 88:1290–1300.

Renner, S. S., and K. Meyer. 2001. Melastomeae come full circle: Biogeographic reconstruction and molecular clock dating. Evolution 55:1315–1324.

Ronquist, F., and J. P. Huelsenbeck. 2003. MrBayes 3: Bayesian phylogenetic inference under mixed models. Bioinformatics 19:1572–1574.

Rozefelds, A. C. 1996. *Eucalyptus* phylogeny and history: A brief summary. Tasforests 8:15–26.

Rutschmann, F. 2005. Bayesian molecular dating using paml/multidivtime. A step-by-step manual. Version 1.5 (July 2005). Institute of Systematic Botany, University of Zurich, Zurich, Switzerland. Available from http://www.plant.ch.

Rutschmann, F. 2006. Molecular dating of phylogenetic trees: A brief review of current methods that estimate divergence times. Diversity Distrib. 12:35–48.

Rutschmann, F., T. Eriksson, J. Schönenberger, and E. Conti. 2004. Did Crypteroniaceae really disperse out of India? Molecular dating evidence from *rbcL*, *ndhF*, and *rpl*16 sequences. Int. J. Plant Sci. 165:69–83.

Sanderson, M. J. 1997. A nonparameteric approach to estimating divergence times in the absence of rate constancy. Mol. Biol. Evol. 14:1218–1231.

Sanderson, M. J. 1998. Estimating rate and time in molecular phylogenies: Beyond the molecular clock? Pages 242–264 *in* Molecular systematics of plants II; DNA sequencing (D. E. Soltis, P. S. Soltis, and J. J. Doyle, eds.). Kluwer Academic Publishers, Norwell, Massachusetts.

Sanderson, M. J. 2002. Estimating absolute rates of molecular evolution and divergence times: A penalized likelihood approach. Mol. Biol. Evol. 19:101–109.

Sanderson, M. J. 2003. r8s: Inferring absolute rates of molecular evolution and divergence times in the absence of a molecular clock. Bioinformatics 19:301–302.

Sanderson, M. J., J. L. Thorne, N. Wikström, and K. Bremer. 2004. Molecular evidence on plant divergence times. Am. J. Bot. 91:1656–1665.

Schönenberger, J., and E. Conti. 2003. Molecular phylogeny and floral evolution of Penaeaceae, Oliniaceae, Rhynchocalycaceae, and Alzateaceae (Myrtales). Am. J. Bot. 90:293–309.

Sebola, R. J., and K. Balkwill. 1999. Resurrection of two previously confused species, *Olinia capensis* (Jacq.) Klotzsch and *O. micrantha* Decne. (Oliniaceae). S. Afr. J. Bot. 65:97–103.

Smith, A. B., and J. J. Peterson. 2002. Dating the time of origin of major clades: Molecular clocks and the fossil record. Rev. Earth Panet. Sci. 30:65–88.

Soltis, P. S., D. E. Soltis, V. Savolainen, P. R. Crane, and T. G. Barraclough. 2002. Rate heterogeneity among lineages of tracheophytes: Integration of molecular and fossil data and evidence for molecular living fossils. Proc. Natl. Acad. Sci. USA 99:4430–4435.

Springer, M. S. 1995. Molecular clocks and the incompleteness of the fossil record. J. Mol. Evol. 41:531–538.

Storey, M., J. J. Mahoney, A. D. Saunders, R. A. Duncan, S. P. Kelley, and M. F. Coffin. 1995. Timing of hot spot-related volcanism and the breakup of Madagascar and India. Science 267:852–855.

Swofford, D. L. 2001. PAUP* 4.0b10: Phylogenetic analysis using parsimony (*and other methods), version 4.0b10. Sinauer Associates, Sunderland, Massachusetts.

Sytsma, K. J., A. Litt, M. L. Zjhra, J. C. Pires, M. Nepokroeff, E. Conti, J. Walker, and P. G. Wilson. 2004. Clades, clocks, and continents:

Historical and biogeographical analysis of Myrtaceae, Vochysiaceae, and relatives in the southern hemisphere. Int. J. Plant Sci. 165:85–105.

Tavaré, S., C. R. Marshall, O. Will, C. Soligo, and R. D. Martin. 2002. Using the fossil record to estimate the age of the last common ancestor of extant primates. Nature 416:726–729.

Thompson, J. D., T. J. Gibson, F. Plewniak, F. Jeanmougin, and D. G. Higgins. 1997. The ClustalX windows interface: Flexible strategies for multiple sequence alignment aided by quality analysis tools. Nucleic Acids Res. 24:4876–4882.

Thorne, J. L., and H. Kishino. 2002. Divergence time and evolutionary rate estimation with multilocus data. Syst. Biol. 51:689–702.

Thorne, J. L., H. Kishino, and I. S. Painter. 1998. Estimating the rate of evolution of the rate of molecular evolution. Mol. Biol. Evol. 15:1647–1657.

Tobe, H., and P. H. Raven. 1984. The embryology and relationships of Oliniaceae. Plant Syst. Evol. 146:105–116.

van der Hammen, T. 1954. El desarrollo de la flora colombiana en los periodos geológicos. I. Maestrichtiano hasta Terciario más inferior. Boletín de Geología 2:49–106.

van Tuinen, M., and E. A. Hadly. 2004. Error in estimation of rate and time inferred for the early amniote fossil record and avian molecular clocks. J. Mol. Evol. 59:267–276.

Welch, J. J., and L. Bromham. 2005. Molecular dating when rates vary. Trends Ecol. Evol. 20:320–327.

Wikström, N., V. Savolainen, and M. W. Chase. 2001. Evolution of the angiosperms: Calibrating the family tree. Proc. R. Soc. B 268:2211–2220.

Wikström, N., V. Savolainen, and M. W. Chase. 2003. Angiosperm divergence times: Congruence and incongruence between fossils and sequence divergence estimates. Pages 142–165 in Telling the evolutionary time: Molecular clocks and the fossil record (P. C. J. Donoghue and M. P. Smith, eds.). Taylor & Francis, London, UK.

Wilson, P. G., M. M. O'Brien, M. M. Heslewood, and C. J. Quinn. 2005. Relationships within Myrtaceae sensu lato based on a matK phylogeny. Plant Syst. Evol. 251:3–19.

Wray, G. A. 2001. Dating branches on the Tree of Life using DNA. Genome Biol. 3:1.1–1.7.

Yang, Z. 2004. A heuristic rate smoothing procedure for maximum likelihood estimation of species divergence times. Acta Zool. Sin. 50:645–656.

Yang, Z., and B. Rannala. 2005. Bayesian estimation of species divergence times under a molecular clock using multiple fossil calibrations with soft bounds. Mol. Biol. Evol. 23:212–226.

Yoder, A. D., and M. D. Nowak. 2006. Has vicariance or dispersal been the predominant biogeographic force in Madagascar? Only time will tell. Annu. Rev. Ecol. Evol. Syst. 37:405–431.

Zuckerkandl, E., and L. Pauling. 1965. Evolutionary divergence and convergence in proteins. Pages 97–166 in Evolving genes and proteins (V. Bryson, and H. Vogel, eds.). Academic Press, New York.

Zurawski, G., B. Perrot, W. Bottomley, and P. R. Whitfield. 1981. The structure of the gene for the large subunit of ribulose-1,5-bisphosphate carboxylase from spinach chloroplast DNA. Nucleic Acids Res. 14:3251–3270.

APPENDIX 1

Fossil Nodal Assignment

No reliable fossils are available for Crypteroniaceae (Conti et al., 2002). Small heterocolpate pollen grains from the Upper Miocene (about 11 My old) found in Northwest Borneo cannot be unequivocally attributed to Crypteroniaceae, because this fossil pollen type is also typical of Melastomataceae, Penaeaceae, Oliniaceae, and Combretaceae (Anderson and Muller, 1975; Muller, 1975, 1981). After carefully reviewing the paleobotanic literature of Myrtales, six fossils were selected for calibration in molecular dating analyses (see Table 1 and Fig. 1). Based both on their morphological characters and previous

nodal assignments in published phylogenies (Melastomataceae: Clausing and Renner, 2001; Renner et al., 2001; Renner and Meyer, 2001; Renner, 2004; Myrtaceae: Sytsma et al., 2004; Onagraceae: Berry et al., 2004), five out of the six fossils could justifiably be assigned to different nodes.

Fossil 1.—Fossil 1 is represented by leaves from the Early Eocene (53 My) of North Dakota (Table 1). Hickey (1977), who first described them, stated that they resemble most closely the leaves of extant Miconieae and Merianieae, but assessed that "they all differ, however, in not being deeply cordate and in having tertiaries which do not form a good V pattern." Renner et al. (2001) further confirmed the resemblance with leaves of modern Miconieae and Merianieae. However, because all Melastomataceae, including *Pternandra*, share the same basic kind of acrodromous leaf venation, Renner et al. (2001) decided to assign the fossils to the entire Melastomataceae crown group (node 1a in the present study; see Fig. 1), a view later shared by Sytsma et al. (2004) in a Myrtales-wide dating analysis. Conversely, in the light of the stated similarities with Miconieae and Merianieae and the known temporal gap between lineage divergence and first appearance of a synapmorphy in the fossil record, Conti et al. (2002), Morley and Dick (2003), and Rutschmann et al. (2004) decided to assign the fossil leaves either to the stem (node 1b) or to the crown group (node 1c) that includes Miconieae and Merianieae (Fig. 1). Renner (2004) included both assignment possibilities in subsequent Bayesian dating analyses of Melastomataceae. In summary, the Miocene leaves of Melastomataceae can be defensibly assigned to three different nodes (1a, 1b, and 1c; see Fig. 1). Because the branch separating node 1a and 1b is long, fossil assignments above or below this branch was expected to strongly influence the dating results.

Fossil 2.—Fossil 2 is represented by fossil seeds from Miocene deposits in Siberia, the Tambov region, Belarus, Poland, several sites in Germany, and Belgium (23 to 26 My, Dorofeev, 1960, 1963, 1988; Collinson and Pingen, 1992; Dyjor et al., 1992; Fairon-Demaret, 1994; Mai, 1995, 2000; Table 1). These seeds are most similar to those of extant members of Osbeckieae and Rhexieae (now Melastomeae; Clausing and Renner, 2001), but differ in several significant features, especially the presence of multicellular tubercles (Collinson and Pingen, 1992). Renner and Meyer (2001) assigned the fossils to the crown group of Melastomeae, because "this kind of testa ornamentation is synapomorphic for the *Rhexia-Arthrostemma-Pachyloma* subclade of Melastomeae." Renner et al. (2001), Conti et al. (2002), Rutschmann et al. (2004), Renner (2004), and Sytsma et al. (2004) all followed this interpretation, although it is difficult to establish with certainty whether these fossils should be assigned to the base of the Melastomeae crown group or to more recent nodes in the tribe. Given our current taxon sampling, the only possible assignment of fossil 2 was to the crown group of Melastomeae, as in previous studies (Fig. 1).

Fossil 3.—Fossil 3 is represented by the pollen *Myrtaceidites lisamae* (syn. *Syncolporites lisamae*) from the Santonian of Gabon (86 My; Herngreen, 1975; Boltenhagen, 1976; Muller, 1981; Table 1). This pollen type was also found in the lower Senonian of Borneo (Muller, 1968) and the Maastrichtian of Colombia (van der Hammen, 1954). Sytsma et al. (2004) attributed this pollen to the crown group of Myrtaceae s.s. (corresponding to node 3c in Fig. 1), but pollen grains of Myrtaceae s.s. and Psiloxyloideae (Wilson et al., 2005) are difficult to distinguish. Therefore, a minimal age of 86 mys can be assigned to three different nodes: 3a (stem lineage of Myrtaceae s.l.), 3b (crown group of Myrtaceae s.l. or stem lineage of Myrtaceae s.s.), and 3c (crown group of Myrtaceae s.s.; Fig. 1). Again, because the branch separating nodes 3a and 3b is long, different assignments were expected to have a relevant impact on the dating results.

Fossil 4.—Fossil 4 is represented by fruits and seeds of *Paleomyrtinaea* from the Late Paleocene of North Dakota (56 mys; Crane et al., 1990; Pigg et al., 1993; Table 1). Samples attributed to *Paleomyrtinaea* were also found in the Early Eocene of British Columbia (54 My; Manchester, 1999). These fruits and seeds have seed coat features (Lantern and Sharp, 1989) and an unornamented C-shape embryo (Lantern and Stevenson, 1986) that resemble those of the largely American subtribe Myrtinae, included in Myrteae (Pigg et al., 1993). Sytsma et al. (2004) assigned the fossil to the crown group of the Myrteae (corresponding to node 4b in Fig. 1), because Myrtinae proved to be paraphyletic in their phylogenetic analysis. As our taxon sampling includes two members of Myrteae that do not represent subtribe Myrtinae, we decided to assign fossil 4 either to the Myrteae crown group (node 4b; as in Sytsma

et al., 2004) or the Myrteae stem lineage (node 4a; Fig. 1). The branch separating nodes 4a and 4b is short, thus alternative calibrations were not expected to have large effects on nodal age estimates.

Fossil 5.—Fossil 5 is represented by the earliest Eucalypt-like fruits from the Middle Eocene Redbank Plains Formation in South Eastern Queensland, Australia (Rozefelds, 1996; discovered by Robert Knezour in 1990; pers. comm. David Greenwood, Brandon University, Manitoba, Canada; Table 1). Similar fossil fruits were found in the Middle Eocene sediments near lake Eyre, Nelly Creek, in northern South Australia (Christophel et al., 1992). Both fossils provide a minimum age of 48 My for the most recent common ancestor (MRCA) of *Eucalyptus* and *Angophora* (node 5b). Alternatively, we assigned the fossil to the stem lineage of Eucalypteae (node 5a; Fig. 1), because the observed type of capsule is also similar to the fruit of other taxa in Eucalypteae (Rozefelds, 1996). As for fossil 4, the branch separating nodes 5a and 5b is short, thus alternative calibrations were not expected to have large effects on nodal age estimates.

Fossil 6.—Fossil 6 is represented by the pollen *Diporites aspis* from the Early Oligocene (33.7 to 28.5 My) of Otway Basin (Australia), described by Berry et al. (1990; Table 1). Comparisons of the fossil pollen with extant members of *Fuchsia* (Daghlian et al., 1985) left no question that *Diporites aspis* represents pollen of *Fuchsia*. Molecular clock analyses of a *Fuchsia* phylogeny calibrated with non-*Fuchsia* fossils resulted in an estimated age interval for the *Fuchsia* crown group that was consistent with the paleobotanical age of *Diporites aspis* (Berry et al., 2004; Sytsma et al., 2004). We therefore assigned a minimal age of 28.5 My to

the *Fuchsia* crown group (node 6b). Alternatively, we assigned the age of the fossil to the *Fuchsia* stem lineage (node 6a; Fig. 1), because the synapomorphies visible in the fossil pollen might have evolved before the diversification of *Fuchsia*, and closer to the stem node representing the phylogenetic split between *Fuchsia* and its sister clade. As for fossils 4 and 5, the branch separating nodes 6a and 6b is short, thus alternative calibrations were not expected to have large effects on nodal age estimates.

Considering all possible assignments of the six fossils reviewed above, 72 different combinations exist, corresponding to 72 calibration sets, each comprising six calibration points (Table 2; Fig. 1). The ages of the six fossils used in each set were assigned as follows: In the fossil cross-validation procedure (see below), we followed the original strategy by Near and Sanderson (2004) and used fixed ages, because the goal of the procedure is to measure the amount of deviation between the fossil and the estimated ages. For fossils 1, 3, 4, and 5 we fixed the corresponding nodes at 53, 86, 56, and 48 My, respectively (Table 1; Fig. 1). For fossils 2 and 6, we used 23 and 28.5 My as minimum constraints and 26 and 33.7 My as maximum constraints, respectively, because age intervals were available from the paleobotanical literature (Table 1; Fig. 1).

In the molecular dating analyses aimed at estimating the age of node X, however, we always assigned the oldest reported age as a minimum constraint to each one of the six calibration points in a set, bearing in mind that fossils always represent minimum ages, due to the gaps in the fossil record (Doyle and Donoghue, 1993; Sanderson, 1998).